MOLECULAR AND CELLULAR BIOLOGY, Dec. 2006, p. 9016–9034 Vol. 26, No. 23
0270-7306/06/$08.00+0 doi:10.1128/MCB.01383-06

Interaction between ROCK II and Nucleophosmin/B23 in the Regulation of Centrosome Duplication▽

Zhiyong Ma,[1] Masayuki Kanai,[1] Kenji Kawamura,[1,2] Kozo Kaibuchi,[3] Keqiang Ye,[4] and Kenji Fukasawa[1]*

Department of Cell Biology, Neurobiology and Anatomy, University of Cincinnati College of Medicine, Cincinnati, Ohio 45267-0521[1]; Department of Urology, Kanazawa Medical University, 1-1 Daigaku Uchinada, Ishikawa, 920-0293, Japan[2]; Nagoya University Graduate School of Medicine, Showa, Nagoya, Aichi 466-8500, Japan[3]; and Department of Pathology and Laboratory Medicine, School of Medicine, Emory University, Georgia 30322[4]

Received 27 July 2006/Returned for modification 1 September 2006/Accepted 13 September 2006

Nucleophosmin (NPM)/B23 has been implicated in the regulation of centrosome duplication. NPM/B23 localizes between two centrioles in the unduplicated centrosome. Upon phosphorylation on Thr^{199} by cyclin-dependent kinase 2 (CDK2)/cyclin E, the majority of centrosomal NPM/B23 dissociates from centrosomes, but some NPM/B23 phosphorylated on Thr^{199} remains at centrosomes. It has been shown that Thr^{199} phosphorylation of NPM/B23 is critical for the physical separation of the paired centrioles, an initial event of the centrosome duplication process. Here, we identified ROCK II kinase, an effector of Rho small GTPase, as a protein that localizes to centrosomes and physically interacts with NPM/B23. Expression of the constitutively active form of ROCK II promotes centrosome duplication, while down-regulation of ROCK II expression results in the suppression of centrosome duplication, especially delaying the initiation of centrosome duplication during the cell cycle. Moreover, ROCK II regulates centrosome duplication in its kinase and centrosome localization activity-dependent manner. We further found that ROCK II kinase activity is significantly enhanced by binding to NPM/B23 and that NPM/B23 acquires a higher binding affinity to ROCK II upon phosphorylation on Thr^{199}. Moreover, physical interaction between ROCK II and NPM/B23 in vivo occurs in association with CDK2/cyclin E activation and the emergence of Thr^{199}-phosphorylated NPM/B23. All these findings point to ROCK II as the effector of the CDK2/cyclin E-NPM/B23 pathway in the regulation of centrosome duplication.

The centrosome is composed of a pair of centrioles and surrounding protein aggregates known as pericentriolar material. The centrosome, as a core component of the spindle pole, plays a key role in the establishment of bipolar spindles during mitosis, which is essential for the accurate segregation of chromosomes to daughter cells (reviewed in references 10 and 13). Upon cytokinesis, each daughter cell inherits only one centrosome; hence, the centrosome must duplicate once in each cell cycle prior to the next mitosis. In animal cells, centrosome duplication proceeds in coordination with other cell cycle events (i.e., DNA synthesis) (27): centrosome duplication begins near the G_1/S boundary and is completed at late G_2. Centrosome duplication begins with the physical separation of paired centrioles, followed by procentriole formation in the vicinity of each preexisting centriole. Initiation of centrosome duplication is triggered by cyclin-dependent kinase 2 (CDK2)/cyclin E (reviewed in reference 18), which is activated in late G_1 primarily by temporal expression of cyclin E (reviewed in references 28 and 35). Several targets of CDK2 in the initiation of centrosome duplication have been identified, including nucleophosmin (NPM)/B23, Mps1, and CP110 (7, 12, 32).

NPM/B23 is a multifunctional protein implicated in a variety of cellular events, including ribosome assembly, pre-rRNA processing (17, 39, 51), mRNA processing (34, 44), DNA duplication through physical interaction with DNA polymerase α and RB (33, 42), nucleocytoplasmic protein trafficking via binding to the nuclear localization signals of target proteins (4, 40, 48), molecular chaperoning (41), and centrosome duplication (15, 32, 38, 46, 49). Analysis of the centrosomal association of NPM/B23 has revealed that NPM/B23 localizes between the paired centrioles, and upon phosphorylation on Thr^{199} by CDK2/cyclin E, the majority of the NPM/B23 proteins dissociate from centrosomes prior to the initiation of centrosome duplication (separation of paired centrioles), implicating NPM/B23 in the pairing of centrioles (38). In this context, NPM/B23 acts as a suppressor of centrosome duplication. Indeed, the down-regulation of NPM/B23 results in the abnormal amplification of centrosomes (15). However, some Thr^{199}-phosphorylated proteins remain at centrosomes and translocate toward a mother centriole of the pair (38), suggesting that those remaining NPM/B23 proteins may be involved in the regulation of centrosome duplication in a manner different from that used in centriole pairing. The interesting feature of NPM/B23 is that it simultaneously exerts different functions through affecting proteins of the different, often seemingly antagonistic, biological pathways/processes. For instance, NPM/B23 can act oncogenically as well as antioncogenically. In cancers, NPM/B23 is frequently mutated or lost, suggesting its role as a tumor suppressor, while NPM/B23 is equally

* Corresponding author. Mailing address: Department of Cell Biology, University of Cincinnati College of Medicine, P.O. Box 670521 (3125 Eden Ave.), Cincinnati, OH 45267-0521. Phone: (513) 558-4939. Fax: (513) 558-4454. E-mail: Kenji.Fukasawa@uc.edu.

▽ Published ahead of print on 2 October 2006.

frequently overexpressed, suggesting its oncogenic role (16). Experimentally, the overexpression of NPM/B23 results in cellular transformation (23), while partial depletion of NPM/B23 in mice accelerates oncogenesis (15). Thus, it would not be surprising if NPM/B23 is involved in the regulation of centrosome duplication in more than one pathway, and such regulatory pathways could either promote or suppress centrosome duplication.

Here, we identified ROCK II, also known as ROKα or Rho(-associated) kinase, as a centrosomal protein that physically interacts with NPM/B23 with a strong affinity. ROCK II is Ser/Thr kinase controlled by the small GTPase Rho (24, 26). We found that ROCK II promotes centrosome duplication in its kinase and centrosome localization activity-dependent manner. Moreover, the kinase activity of ROCK II is markedly enhanced by physical interaction with NPM/B23. Thr^{199}-phosphorylated NPM/B23 has a higher binding affinity to ROCK II than unphosphorylated NPM/B23, and ROCK II-NPM/B23 complex formation in vivo depends on the Thr^{199} phosphorylation of NPM/B23. Thus, the effects of CDK2/cyclin E-mediated phosphorylation of Thr^{199} on the initiation of centrosome duplication is twofold: removing the centriole pairing activity of NPM/B23 and potentiating ROCK II to promote the initiation of centrosome duplication.

MATERIALS AND METHODS

Cells and transfection. NIH 3T3 and mouse skin fibroblasts (MSFs) were maintained in complete medium (Dulbecco's modified Eagle's medium supplemented with 10% fetal bovine serum, penicillin [100 units/ml], and streptomycin [100 μg/ml]) in an atmosphere containing 10% CO_2. Transfection was performed using either Lipofectamine 2000 (Invitrogen) or Fugene-6 (Roche) reagent.

Plasmids and antibodies. Generation of the ROCK II mutants (with the catalytic domain [CAT], the coiled-coil domain [coil], RB, and the pleckstrin homology domain [PH]) was previously described (2). Other ROCK II mutants were generated by the PCR-based method. Glutathione *S*-transferase (GST)–ROCK II and GST-CAT used for in vitro kinase assay were prepared from sf9 insect cells as described previously (26). GST-ROCK II (or -CAT) and His_6^+-NPM/B23 proteins were bacterially purified using glutathione Sepharose 4B (Pharmacia Biotech) and Ni-nitrilotriacetic acid resins (QIAGEN), respectively. For generation of the plasmid encoding small interfering RNA (siRNA) specific for ROCK II, the sequence 5′-GGAACTGCAAGACCAACTT-3′ (corresponding to cDNA sequence positions 2580 to 2598) was cloned into the pSUPER vector (OligoEngine). For generation of the plasmid encoding siRNA specific for NPM/B23, 5′-AGAACGGTCAGTTTAGGAG-3′ (corresponding to cDNA sequence positions 133 to 151 [5]) was cloned into the pSUPER vector.

The antibodies used in this study were anti-ROCK II polyclonal (07-443; Upstate Biotechnology), anti-ROCK II monoclonal (610623; BD Biosciences), anti-ROCK I polyclonal (sc-5560; Santa Cruz), anti-NPM/B23 monoclonal (51), anti-NPM/B23 polyclonal (generated in our laboratory [38]), anti-GST (Z-5) polyclonal (sc-459; Santa Cruz), anti-FLAG monoclonal (M2; Sigma), anti-γ-tubulin monoclonal (GTU-88; Sigma), anti-γ-tubulin polyclonal (generated in our laboratory), anticentrin monoclonal (36), anti-GFP monoclonal (1814460; Roche), anti-phospho-Ser^{19} MLC 2 polyclonal (3671; Cell Signaling), anti-MLC 2 polyclonal (sc-15370; Santa Cruz), anti-His tag monoclonal (Ab-1; Oncogene Science), antivimentin polyclonal (AB994; Chemicon), anti-cyclin E polyclonal (M-20; Santa Cruz), and anti-β-tubulin monoclonal (TUB2.1; Sigma) antibodies.

GST-NPM/B23 affinity purification of centrosomal proteins. Centrosomes were isolated as described previously (29, 32). Centrosomes are denatured in 9 M urea to dissociate centrosomal components and then subjected to renaturation by dialysis against the buffer solution (20 mM Tris-Cl [pH 7.4], 25 mM NaCl, 5 mM $MgCl_2$, 1 mM EDTA, 1 mM ATP, 1 mM GTP, 0.01% NP-40, 2 μg/ml leupeptin, 2 μg/ml aprotinin, 1 mM phenylmethylsulfonyl fluoride [PMSF]) at 4°C. At 6 h of dialysis, bacterially purified GST-NPM/B23 or a GST control was added, and the samples were further dialyzed for 12 h. GST-NPM/B23 and associating proteins were pulled down using glutathione Sepharose 4B, washed in the buffer (20 mM Tris-Cl [pH 7.4], 80 mM NaCl, 5 mM $MgCl_2$, 1 mM EDTA, 10% glycerol) five times, resolved in a 6 to 15% gradient of sodium dodecyl sulfate-polyacrylamide gel electrophoresis (SDS-PAGE) gel, and silver stained. The bands of interest were excised, and subjected to mass spectrometric analysis as described previously (32).

In vitro protein binding assay. His_6^+-NPM/B23 and GST-ROCK II (wild-type and mutant) proteins were incubated in the binding buffer (50 mM Tris-Cl [pH 7.5], 1 mM $MgCl_2$, 0.1 mM ATP, 10% glycerol, 0.1 μg/μl bovine serum albumin, 2 μg/ml leupeptin, 2 μg/ml aprotinin, 1 mM PMSF) for 2 h at 4°C. GST affinity beads were added and incubated for an additional 2 h. After extensive washes with the wash buffer (50 mM Tris-Cl [pH 7.5], 1 mM $MgCl_2$, 0.1 mM ATP, 50 mM NaCl, 10% glycerol, 1% Tween 20), the precipitates were resolved by SDS-PAGE and subjected to immunoblot analysis.

Immunoblotting and immunoprecipitation. For immunoblot analysis, cells were lysed in SDS–NP-40 lysis buffer (1% SDS, 1% NP-40, 50 mM Tris [pH 8.0], 150 mM NaCl, 2 μg/ml leupeptin, 2 μg/ml aprotinin, 1 mM PMSF). The lysates were boiled for 5 min and cleared by centrifugation at 4°C. The samples were denatured in sample buffer (2% SDS, 10% glycerol, 60 mM Tris [pH 6.8], 5% β-mercaptoethanol, 0.01% bromophenol blue), resolved by SDS-PAGE, and transferred onto an Immobilon-P membrane (Millipore). The blots were incubated in blocking buffer (5% [wt/vol] nonfat dry milk in Tris-buffered saline plus Tween 20) for 1 h and incubated with primary antibodies for 16 h at 4°C. After extensive washing in Tris-buffered saline plus Tween 20, the blots were incubated with horseradish peroxidase-conjugated secondary antibodies for 1 h at room temperature. The antibody-antigen complex was visualized by ECL chemiluminescence (Amersham Pharmacia). Quantification was performed with Quantity One software (Bio-Rad). For immunoprecipitation, cells were lysed in NP-40 lysis buffer (50 mM Tris-HCl [pH 7.5], 50 mM β-glycerophosphate, 150 mM NaCl, 5 mM $MgCl_2$, 10 mM EGTA, 5 mM NaF, 1% Na deoxycholate, 1% NP-40, 2 μg/ml leupeptin, 2 μg/ml aprotinin, 1 mM PMSF). The lysates were precleared by incubation with protein G-agarose beads for 1 h at 4°C, and incubated with antibodies overnight at 4°C. The immuno-complexes were collected by protein G agarose beads, washed in ice-cold NP-40 lysis buffer, boiled in sample buffer, and resolved by SDS-PAGE.

In vitro kinase assay. GST-ROCK II or GST-CAT purified from sf9 cells or immunoprecipitates from cells transfected with GFP-ROCK II mutants using anti-GFP antibody were subjected to a kinase reaction in a buffer (50 mM Tris-Cl [pH 7.5], 1 mM $MgCl_2$, 5 mM NaF, 2 μg/ml leupeptin, 2 μg/ml aprotinin, 1 mM PMSF) with a substrate (0.15 μg/μl of vimentin) in the presence of [γ-^{32}P]ATP and incubated for 30 min at 30°C. For examination of the kinase activities of CDK2/cyclin E, the lysates were subjected to immunoprecipitation using anti-cyclin E antibody. The antibody-antigen complexes were collected with protein A-agarose beads, and tested for a histone H1 kinase activity as described previously (30). The kinase activity was quantified using a Fuji phosphorimager.

Indirect immunofluorescence. Cells were fixed with 10% formalin–10% methanol. For examination of the centrosomal localization of ROCK II, cells were briefly extracted with 0.1% Triton X-100 in phosphate-buffered saline (PBS) for 1 min, followed by extensive washing with PBS prior to fixation. Without a brief extraction, ROCK II signals at centrosomes are heavily masked by the ubiquitous presence of ROCK II, especially when GFP-tagged ROCK II is introduced. Cells were then blocked by 10% normal goat serum in PBS for 1 h and incubated with antibodies for 1 h. Cells were then incubated with secondary antibodies for 1 h and counterstained for DNA with 4′, 6-diamidino-2-phenylindole (DAPI). Cells were examined under a fluorescence microscope (Nikon Microphot-FX) using a 60× objective lens. The images were captured with a SPOT charge-coupled-device camera (Diagnostic Instruments).

BrdU incorporation assay. The entire procedure was performed using a cell proliferation assay kit (Amersham) as instructed by the supplier. Briefly, after incubation in the labeling medium containing 5-bromo-2′-deoxyuridine (BrdU), cells were washed with PBS and fixed with acetic acid-ethanol. After being blocked with 3% bovine serum albumin in PBS plus 0.1% Tween 20), cells were probed with anti-BrdU monoclonal antibody and detected with fluorescein isothiocyanate-conjugated goat anti-mouse immunoglobulin G2a (IgG2a).

RESULTS

ROCK II binds directly to NPM/B23. To identify a centrosomal protein(s) that interacts with NPM/B23, we isolated centrosomes from NIH 3T3 cells by discontinuous sucrose gradient centrifugation as described previously (29, 32). Since the isolated centrosomes exist as "protein aggregates," we first dissociated centrosomal components in 9 M urea. The dissociated centrosomal components were then renatured by dialy-

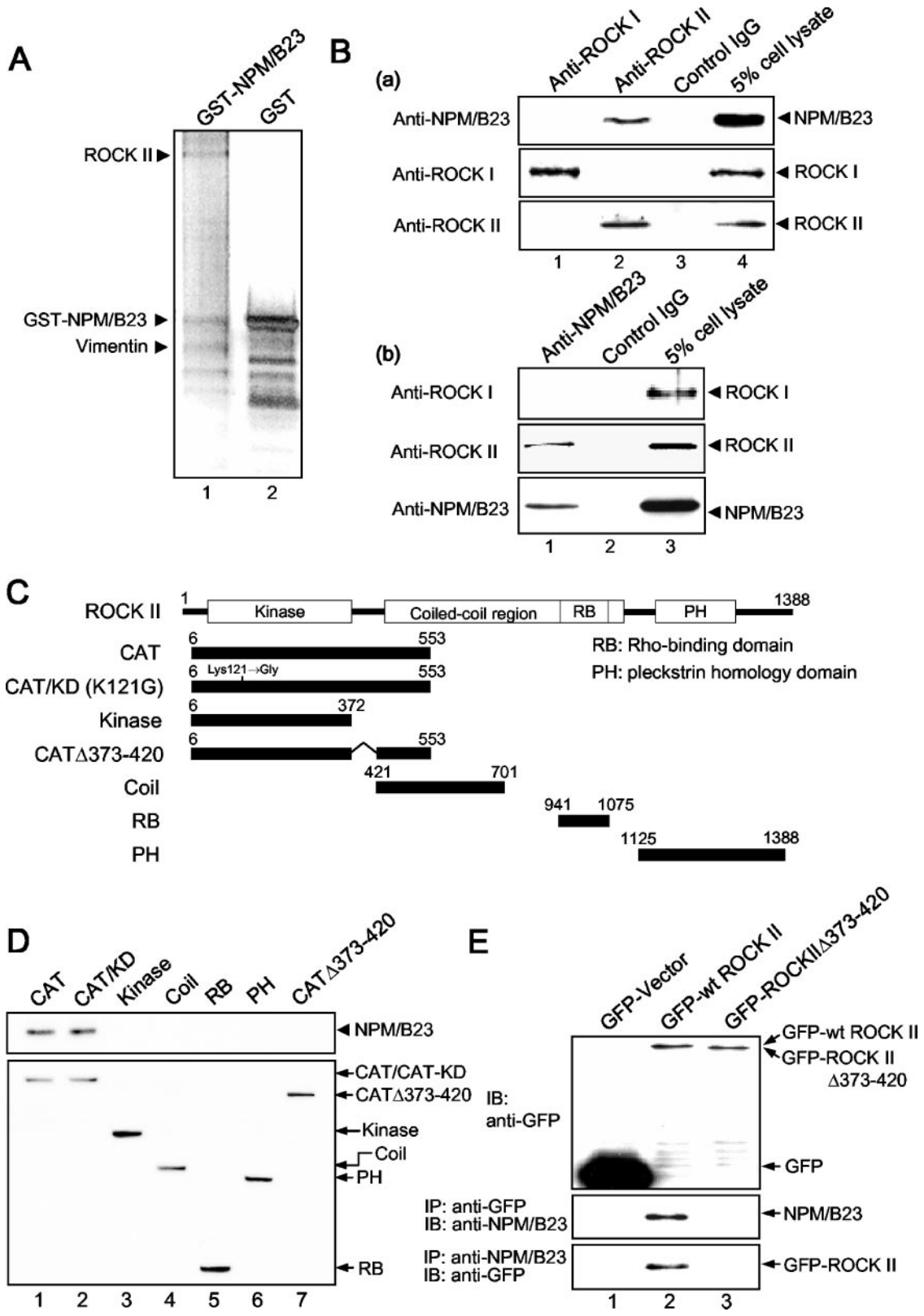

FIG. 1. Physical interaction between NPM/B23 and ROCK II in vitro and in vivo. (A) Identification of ROCK II as an NPM/B23-interacting centrosomal protein. Centrosomes isolated from NIH 3T3 cells were denatured in 9 M urea to dissociate centrosomal components, followed by renaturation. During the renaturing process, the samples were incubated with either GST-NPM/B23 (lane 1) or GST (lane 2) and pulled down with GST affinity beads. The protein complexes were resolved by SDS-PAGE and visualized by silver staining. The protein bands specific to GST-NPM/B23 were excised, subjected to mass spectrometric analysis, and identified as ROCK II and vimentin. (B) Physical interaction between

sis. During the renaturation, GST-NPM/B23 (or GST as a control) was added to the samples. GST-NPM/B23 (or GST) and associating proteins were pulled down with GST affinity beads, resolved by SDS-PAGE, and silver stained (Fig. 1A). This experimental procedure successfully screened the centrosomal proteins that interacted with NPM/B23 with a high affinity and minimized the chaperoning activity-associated background protein binding of NPM/B23. There were two readily distinguishable protein bands (~160 and ~55 kDa) unique to GST-NPM/B23 (lane 1). These proteins were subjected to a mass spectroscopic analysis and identified as ROCK II (160 kDa) and vimentin (55 kDa). ROCK II belongs to a ROCK kinase family consisting of ROCK I and II, which share ~60% homology (31).

We first tested the interaction between NPM/B23 and ROCK II in vivo by coimmunoprecipitation assay using anti-ROCK II and anti-NPM/B23 antibodies (Fig. 1B). Anti-ROCK II antibody coimmunoprecipitated NPM/B23 (Fig.1Ba, top panel, lane 2), and anti-NPM/B23 antibody coimmunoprecipitated ROCK II (Fig. 1Bb, middle panel, lane 1), demonstrating the physical interaction of these two proteins in vivo. Since ROCK I, another member of the ROCK kinase family, also localizes to centrosomes (8), we tested the interaction between ROCK I and NPM/B23. NPM/B23 was not precipitated with anti-ROCK I antibody (Fig.1Ba, top panel, lane 1), and ROCK I was not precipitated with anti-NPM/B23 antibody (Fig.1Bb, top panel, lane 1). Thus, NPM/B23 does not interact with ROCK I.

To test whether NPM/B23 and ROCK II directly interact with each other, an in vitro binding assay was performed using bacterially purified NPM/B23 and ROCK II. Since ROCK II is too large to be efficiently expressed in a bacterial system, a series of GST-fused deletion mutants that cover distinct functional domains (diagramed in Fig. 1C) were generated: GST-CAT (kinase domain plus part of the coiled-coil domain), GST-CAT/KD (GST-CAT in which Lys^{121} at the ATP-binding motif is replaced by Gly), GST-kinase domain (GST-kinase), GST–coil-coil domain (GST-coil), GST-RB, and GST-PH. These mutants were incubated with His_6^+-NPM/B23 and precipitated with GST affinity beads. The precipitates were then immunoblotted for NPM/B23 (Fig. 1D, top) and GST (bottom). NPM/B23 was coimmunoprecipitated only when it was incubated with GST-CAT (lane 1) and GST-CAT/KD (lane 2), indicating that NPM/B23 directly binds to CAT domain (amino acids [aa] 6 to 553) of ROCK II. Since GST-coil (aa 421 to 701) failed to bind to NPM/B23, the NPM/B23 binding region likely resides within aa 6 to 420. Moreover, GST-kinase (aa 6 to 372) failed to bind to NPM/B23. Thus, the sequence comprising aa 373 to 420 may be critical for ROCK II to bind to NPM/B23. Indeed, GST-CAT with aa 373 to 420 deleted could no longer bind to NPM/B23 in vitro (Fig. 1D, lane 7). Similarly, with green fluorescent protein (GFP)-tagged full-length ROCK II with aa 373 to 420 deleted (GFP–ROCK IIΔ373-420), when expressed in NIH 3T3 cells, anti-GFP antibody failed to coimmunoprecipitate NPM/B23 (Fig. 1E, second panel, lane 3) and anti-NPM/B23 antibody failed to coimmunoprecipitate GFP–ROCK IIΔ373-420 (bottom panel, lane 3).

Characterization of the centrosomal association of ROCK II. We next examined whether ROCK II is present in the isolated centrosomes. The cytoplasmic lysates containing centrosomes prepared from NIH 3T3 cells were subjected to discontinuous sucrose gradient centrifugation, and the resulting fractions were immunoblotted with anti-γ-tubulin and anti-ROCK II antibodies (Fig. 2A). The fractionation pattern of ROCK II paralleled that of γ-tubulin, suggesting the presence of ROCK II at the centrosomes.

We also examined the centrosomal localization of ROCK II by coimmunostaining with anti-ROCK II and anti-γ-tubulin antibodies (Fig. 2B). We detected ROCK II at unduplicated and duplicated centrosomes as well as spindle poles during mitosis. To test the specificity of anti-ROCK II antibody, we generated NIH 3T3 cells whose ROCK II expression was silenced by siRNA. We found that ROCK II could be stably silenced (>95%) (Fig. 2C). Cells whose ROCK II expression was silenced by RNA interference (ROCK II-RNAi cells) and control cells transfected with an siRNA vector with a randomized sequence were coimmunostained for γ-tubulin and ROCK II. The ROCK II antibody-reactive signals were no longer detectable at centrosomes in ROCK II-RNAi cells (representative immunostaining images of ROCK II-RNAi and vector control cells are shown in Fig. 2D), demonstrating the specificity of the anti-ROCK II antibody.

To determine the region of ROCK II critical for centrosomal localization, the fragments of ROCK II described in the legend to Fig. 1C were tagged with GFP (Fig. 3A), transfected into NIH 3T3 cells, and immunostained for γ-tubulin. Interestingly, several regions of ROCK II were found to localize to centrosomes, including the kinase, coil, and PH mutants (immunostaining images of GFP-, GFP-CAT-, and GFP-PH-transfected cells are shown in Fig. 3B). Since the C-terminal PH domain constitutes an autoinhibitory region which folds

NPM/B23 and ROCK II in vivo. The lysates prepared from NIH 3T3 cells were subjected to immunoprecipitation using (a) either anti-ROCK I (lane 1) or ROCK II (lane 2) antibodies (lane 3, a control IgG) and (b) anti-NPM/B23 antibody (lane 1) (lane 2, a control IgG). The immunoprecipitates were then immunoblotted with anti-NPM/B23, anti-ROCK I, and anti-ROCK II antibodies. The cell lysates (5% of the amount used for immunoprecipitation) were included in the analyses. (C) Diagram of ROCK II wild-type and deletion mutants. (D) Identification of the sequence of ROCK II critical for NPM/B23 binding. Bacterially purified His_6^+-NPM/B23 proteins were mixed with bacterially purified GST-CAT (lane 1), -CAT/KD (lane 2), -kinase (lane 3), -coil (lane 4), -RB (lane 5), -PH (lane 6), and –CATΔ373-420 (lane 7). The reaction samples were subjected to precipitation using GST affinity beads and immunoblotted with anti-NPM/B23 antibody (upper panel) and anti-GST antibody (lower panel). (E) In vivo demonstration of the critical sequence of ROCK II for NPM/B23 binding. NIH 3T3 cells were transfected with either GFP-tagged full-length ROCK II or ROCK II with aa 373 to 420 deleted. A GFP vector was transfected as a control. Expression levels of transfected ROCK II proteins were determined by immunoblot (IB) analysis using anti-GFP antibody (top). The lysates were also subjected to coimmunoprecipitation (IP) assay using anti-GFP (middle) and anti-NPM/B23 (bottom) antibodies. The immunoprecipitates were immunoblotted with anti-NPM/B23 as well as anti-GFP antibodies. wt, wild type.

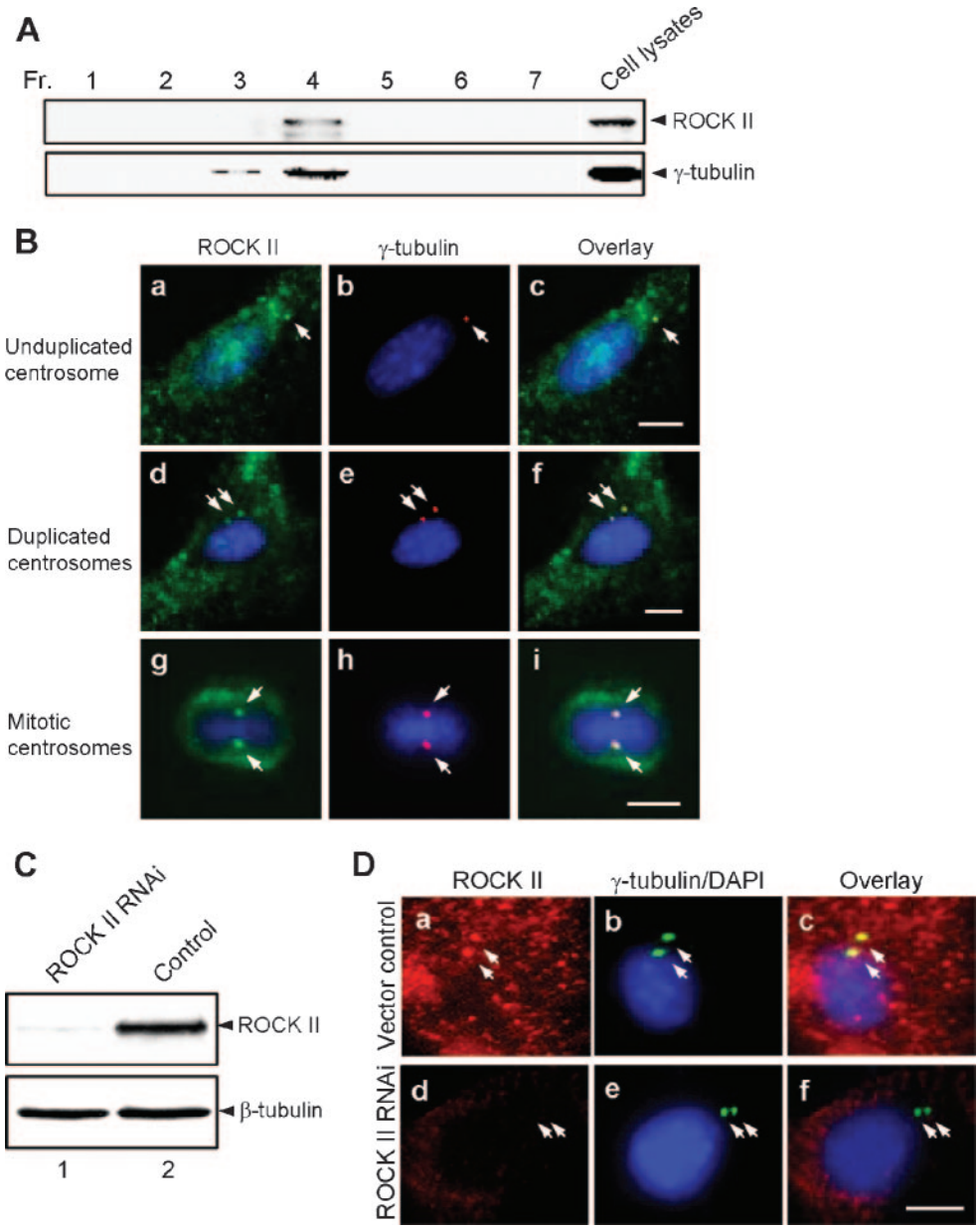

FIG. 2. Localization of ROCK II at centrosomes. (A) Centrosomes were isolated from NIH 3T3 cells by discontinuous sucrose gradient centrifugation, and the resulting fractions were immunoblotted using anti-ROCK II (top) and anti-γ-tubulin (bottom) antibodies. (B) Cells were briefly extracted prior to fixation and coimmunostained with rabbit anti-ROCK II (green) and mouse anti-γ-tubulin (red) antibodies. Cells were also counterstained for DNA with DAPI (blue) and merged with the images of ROCK II and γ-tubulin immunostaining. (a to c) Cell with unduplicated centrosomes; (d to f) cell with duplicated centrosomes; (g to i) mitotic cell. The arrows point to the positions of centrosomes. Scale bar, 10 μm. (C) siRNA-mediated silencing of ROCK II. NIH 3T3 cells were cotransfected with a pSUPER plasmid that encodes siRNA specific for ROCK II (lane 1) and a plasmid encoding a puromycin-resistant gene at a 20:1 molar ratio. The vector (pSUPER with a random sequence of the same nucleotide composition with ROCK II siRNA) was transfected as a control (lane 2). Puromycin-resistant colonies were pooled, and the lysates from the transfectants were immunoblotted with anti-ROCK II (top) and anti-β-tubulin (bottom) antibodies. (D) The ROCK II-RNAi and vector control cells described above were coimmunostained with anti-ROCK II (red) and anti-γ-tubulin (green) antibodies. DAPI-stained images (blue) were merged with the images of γ-tubulin immunostaining. (c and f) Merged images of ROCK II, γ-tubulin, and DNA staining. The arrows point to the positions of centrosomes. Scale bar, 10 μm.

back to interact with the N-terminal kinase domain (1, 6), it is possible that GFP-kinase and GFP-PH may bind to the PH and kinase domains of endogenous ROCK II, respectively. To test this, GFP-tagged ROCK II fragments were transfected into the ROCK II-RNAi cells and examined for their abilities to localize to centrosomes (immunostaining images of GFP-CAT and GFP-PH transfectants are shown in Fig. 3Ca to f). As suspected, both GFP-kinase and GFP-PH failed to localize to centrosomes in the ROCK II-RNAi cells, indicating that GFP-kinase and GFP-PH localize to centrosomes via interaction

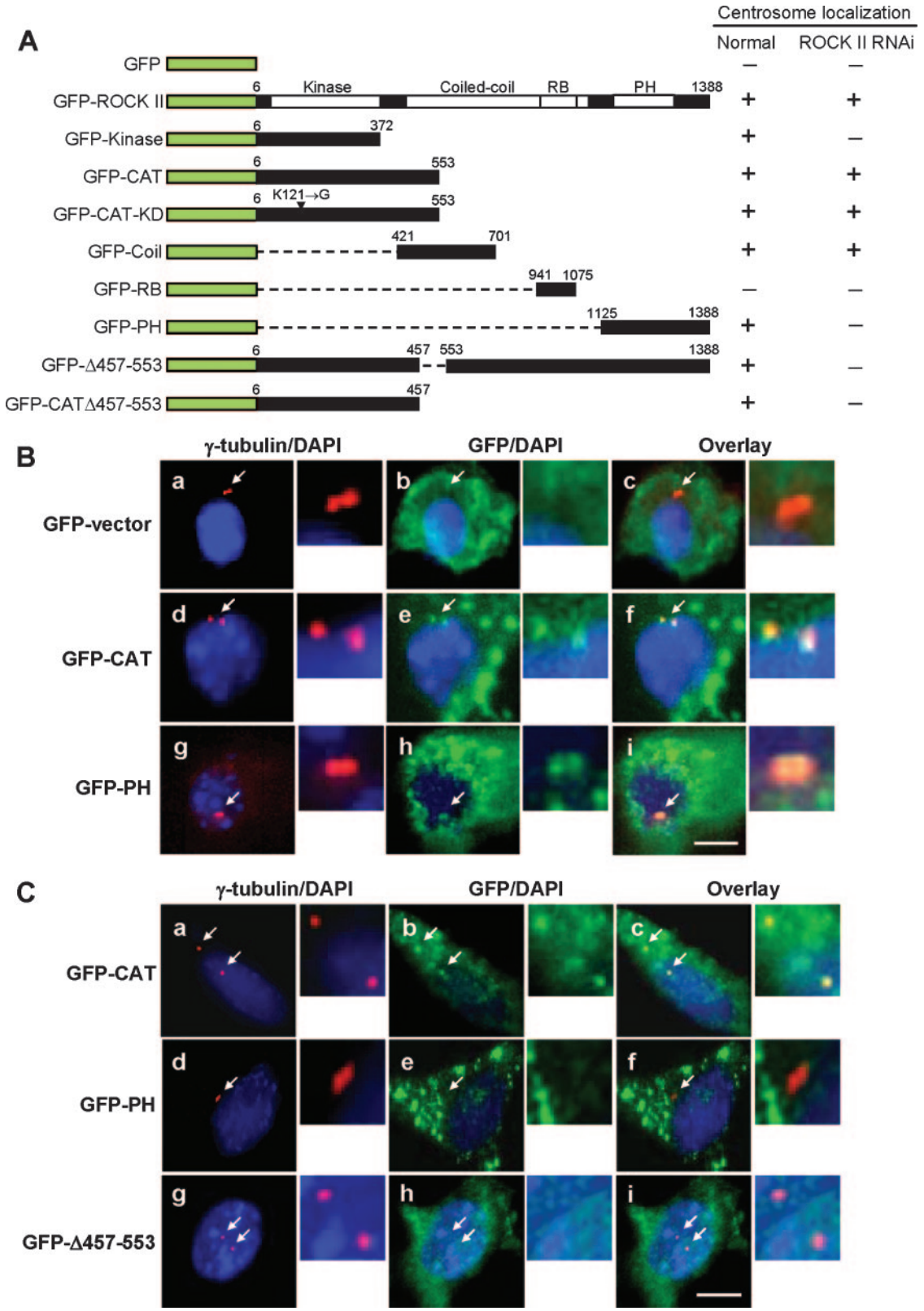

FIG. 3. Characterization of the centrosome-binding activity of ROCK II. (A) Wild-type ROCK II and deletion mutants were tagged with GFP and transfected into NIH 3T3 and ROCK II-RNAi cells. A GFP vector was transfected as a control. At 36 h posttransfection, cells were briefly extracted, fixed and immunostained for γ-tubulin, and examined for the centrosomal localization of GFP-tagged ROCK II proteins, and results are summarized to the right of the diagram. (B) Representative images of the GFP-, GFP-CAT-, and GFP-PH-transfected NIH 3T3 cells. (C) GFP-CAT-, GFP-PH-, and GFP–Δ457-553-transfected ROCK II-RNAi cells. DAPI-stained images (blue) were laid over γ-tubulin- and GFP-immunostained images. The arrows point to the positions of centrosomes. The panel to the right of each image shows the magnified image of the area indicated by arrows. Scale bar, 10 μm.

with endogenous ROCK II. In contrast, GFP-coil and GFP-CAT were still able to localize at centrosomes, indicating that the part of the coiled-coil domain shared by these two ROCK II fragments (aa 421 to 553) may be critical for the centrosome-binding activity of ROCK II. Further deletion within this sequence narrowed it down to aa 457 to 553. For instance, deletion of aa 457 to 553 of full-length ROCK II (GFP–Δ457-553) as well as the CAT mutant (GFP–CATΔ457-553), although they localized to centrosomes in normal cells through interaction with endogenous ROCK II, abolished the ability to localize to centrosomes in the ROCK II-RNAi cells (immunostaining images of GFP–Δ457-553 are shown in Fig. 3Cg to i). It should be noted here that GFP–Δ457-553 as well as GFP–CATΔ457-553 lack the sequence targeted by siRNA used for silencing ROCK II expression. In addition, GFP-CAT/KD localizes to centrosomes (data not shown), indicating that centrosome binding of ROCK II is independent of its kinase activity. The centrosome-binding activities of wild-type and mutant ROCK II in normal and ROCK II-RNAi cells are summarized in Fig. 3A.

ROCK II promotes centrosome reduplication. We tested whether ROCK II is involved in the regulation of centrosome duplication by the centrosome reduplication assay. When cells are exposed to DNA synthesis inhibitors such as aphidicolin (Aph), centrosomes continue to duplicate without DNA synthesis, resulting in centrosome amplification (the presence of three or more centrosomes) (3). However, this phenomenon preferentially occurs in cells with an impaired p53-dependent checkpoint. In the presence of functional p53, p21 CDK inhibitor is up-regulated in a p53-dependent manner in response to the stress associated with exposure to DNA synthesis inhibitors (43), which in turn inhibits CDK2/cyclin E, a known initiator of centrosome duplication. NIH 3T3 cells carried in our laboratory are partially defective in the p53-dependent checkpoint function: they fail to up-regulate p21 upon exposure to Aph, making cells permissive for centrosome reduplication during Aph-induced arrest. ROCK II has an autoinhibitory C-terminal region that binds to the N-terminal kinase region. The kinase is activated when the negative regulatory interaction between these two domains is disrupted by Rho binding to a C-terminal region (1, 6, 19). Thus, deletion of the C-terminal region constitutively activates ROCK II, as is the case for the CAT mutant (Fig. 1C). We transfected GFP-CAT, GFP-CAT/KD, and a control GFP vector into NIH 3T3 cells prearrested by exposure to Aph for 24 h. Transfecting the pre-Aph-arrested cells eliminates the possibility of misinterpretation of data due to the potential alteration of cell cycle progression by the forced expression of GFP-CAT. The GFP-CAT transfectants showed a membrane blebbing typical of the constitutive activation of ROCKs (Fig.4Bc), which is attributed to the ROCK-mediated phosphorylation of myosin light chain 2 (MLC2) (9, 37). Such morphological change was not observed in the control GFP vector (Fig.4Ba) or CAT/KD transfectants (not shown). After transfection, cells continued to be exposed to Aph for 36 h. Over 75% of the GFP-CAT-transfected cells underwent centrosome reduplication, which is significantly higher than that in the vector-transfected cells (~45%) (Fig. 4A; representative immunostaining images of GFP-CAT- and vector-transfected cells are shown in Fig. 4Ba to d). Expression of GFP-CAT/KD resulted in a substantial decrease in the frequency of centrosome amplification (~30%) compared with that in the vector-transfected cells, suggesting that GFP-CAT/KD may act in a dominant negative manner. Furthermore, addition of the ROCK kinase inhibitor Y-27632 (21) immediately after transfection suppressed the promotion of centrosome reduplication by GFP-CAT (Fig. 4A; representative immunostaining images are shown in Fig. 4Be and f). Thus, expression of the CAT mutant accelerates centrosome reduplication under Aph-induced arrest in its kinase activity-dependent manner. We also tested the centrosome duplication regulatory role of ROCK II in U2OS human cells, and we obtained similar results (data not shown). Thus, the involvement of ROCK II in the regulation of centrosome duplication is neither species nor cell type specific.

ROCK II requires its centrosome-binding activity to promote centrosome reduplication. The GFP-CAT mutant with aa 457 to 553 deleted (GFP–CATΔ457-553) can no longer localize to centrosomes (Fig. 3A). To test whether GFP–CATΔ457-553 retains its kinase activity, NIH 3T3 cells were transfected with the GFP vector control, GFP-CAT, or GFP–CATΔ457-553. The lysates prepared from the transfectants were subjected to immunoprecipitation using anti-GFP antibody. The immunoprecipitated GFP, GFP-CAT, and GFP–CATΔ457-553 were then tested for their in vitro kinase activity as described previously (20) using vimentin as the substrate, which is one of the known physiological substrates of ROCK II (14) (Fig. 5A). Similar levels of GFP-CAT and GFP–CATΔ457-553 were immunoprecipitated (Fig. 5A, top). The in vitro kinase assay showed that both GFP-CAT and GFP–CATΔ457-553 phosphorylated vimentin at similar efficiencies (Fig. 5A, middle), demonstrating that GFP–CATΔ457-553 retains full kinase activity.

We also tested whether the kinase activity of GFP–CATΔ457-553 is retained in vivo. It has been shown that ROCK II phosphorylates MLC2 at Ser^{19}, and Ser^{19} phosphorylation of MLC2 can serve as an indicator of the in vivo ROCK II activity (1, 47), although the increase in the levels of phospho-Ser^{19} MLC2 may also be attributed to the inhibition of MLC phosphatase by ROCK II (11, 22). We transfected GFP, GFP-CAT, or GFP–CATΔ457-553 into NIH 3T3 cells. Immunoblot analysis of the lysates prepared from the transfectants with anti-GFP antibody showed that GFP-CAT and GFP–CATΔ457-553 were expressed at similar levels (Fig. 5B, top). The lysates were then immunoblotted with anti-phospho-Ser^{19} MLC2 antibody as well as anti-MLC2 antibody, which detects total MLC2 protein. There was no difference in the levels of total MLC2 among the transfectants (Fig. 5B, bottom), while the level of Ser^{19}-phosphorylated MLC2 was noticeably increased in the GFP-CAT-transfected cells (Fig. 5B, middle, lane 1) compared with the level in control cells (lane 3). In the cells transfected with GFP–CATΔ457-553, the level of Ser^{19}-phosphorylated MLC2 was similar to those in cells transfected with GFP-CAT (Fig. 5B, middle, lane 2). These results show that the GFP–CATΔ457-553 mutant retains full kinase activity in vivo.

To address whether centrosomal localization is required for ROCK II to promote centrosome duplication, we tested GFP–CATΔ457-553 by the centrosome reduplication assay. We transfected GFP, GFP-CAT, and GFP–CATΔ457-553 into NIH 3T3 cells prearrested by Aph. After transfection, cells

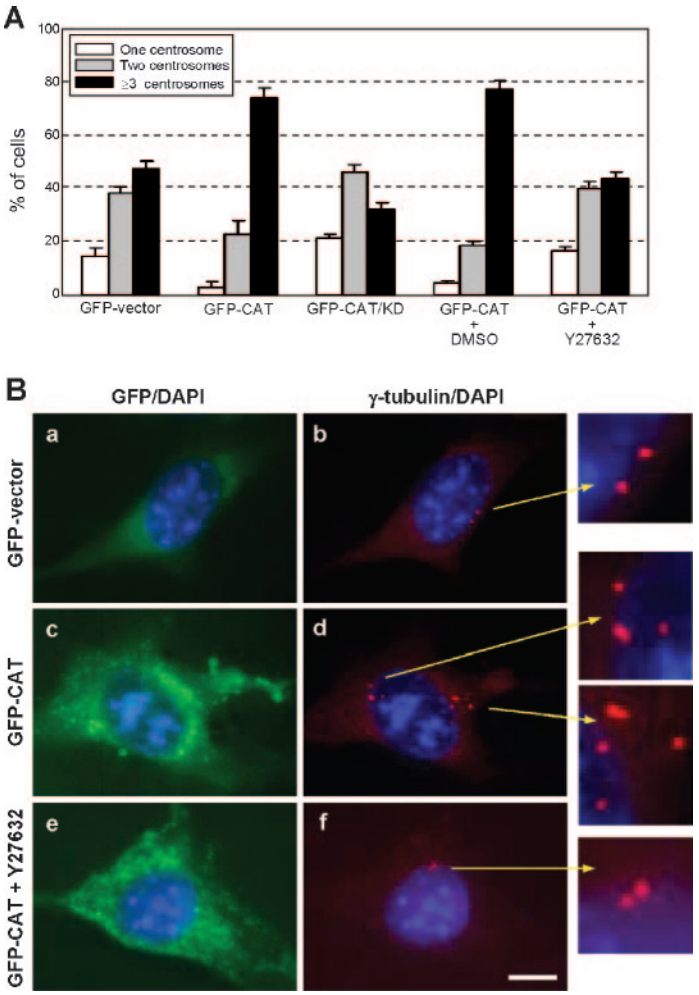

FIG. 4. ROCK II promotes centrosome reduplication. (A) NIH 3T3 cells were first arrested by Aph (2 μg/ml) treatment for 24 h. Cells were then transfected with either the GFP-CAT or the GFP vector in the presence of Aph. After the transfection period (12 h), either the Y-27632 ROCK inhibitor (100 μM) or dimethyl sulfoxide (DMSO) was added to the media in the duplicate GFP-CAT-transfected cell cultures. Cells were fixed at 24 h posttransfection, immunostained for γ-tubulin, and counterstained for DNA with DAPI, and the centrosome profiles of the GFP-positive cells were determined (>300 cells). The results are shown as averages ± standard errors from three independent experiments. (B) Representative immunostained images of vector-transfected cells (a and b) and GFP-CAT-transfected cells (c and d) as well as GFP-CAT-transfected cells in the presence of Y-27632 (e and f) are shown. The panels on the right show the magnified images of the areas indicated by arrows. Scale bar, 10 μm. It should be noted that in this experiment, the cells were directly fixed without preextraction to observe the membrane blebbing associated with the constitutive activation of ROCK II. However, without preextraction, due to the ubiquitous presence of GFP-CAT, the specific localization of GFP-CAT at the centrosomes is highly masked.

continued to be exposed to Aph for 36 h, and the centrosome profiles of the GFP-positive cells were determined (Fig. 5C). As shown in Fig. 4A, expression of GFP-CAT resulted in a high frequency of centrosome amplification (~75%) compared with that in the vector-transfected control cells (~45%). However, the expression of GFP–CATΔ457-553 failed to promote centrosome reduplication; the frequency of centrosome amplification was similar to that of the control cells, indicating that centrosomal localization is critical for ROCK II to promote centrosome reduplication.

ROCK II is required for the timely initiation of centrosome duplication in normal cells. To obtain insight into the role of ROCK II in the regulation of centrosome duplication in normal cells, the ROCK II-RNAi and control cells were exposed to Aph for 60 h, and the centrosome profiles were determined (Fig. 6A; representative immunostaining images are shown in Fig. 6B). The control cells reduplicated centrosomes under Aph-induced arrest, resulting in a frequency of centrosome amplification of ~40% (in this assay, cells were not prearrested by Aph; hence, the total Aph incubation time was shorter than in the other centrosome reduplication assay [see, e.g., Fig. 4A]). In contrast, in ROCK II-RNAi cells, centrosome reduplication was significantly suppressed (~20%). When GFP-CAT which lacks the sequence targeted by siRNA was introduced into the ROCK II-RNAi cells, the suppression of centrosome reduplication was no longer detected, demonstrating that the suppression of centrosome reduplication in the ROCK II-RNAi cells is associated with the down-regulation of ROCK II.

In ROCK II-RNAi cells, centrosome reduplication during Aph-induced arrest was suppressed but was not completely

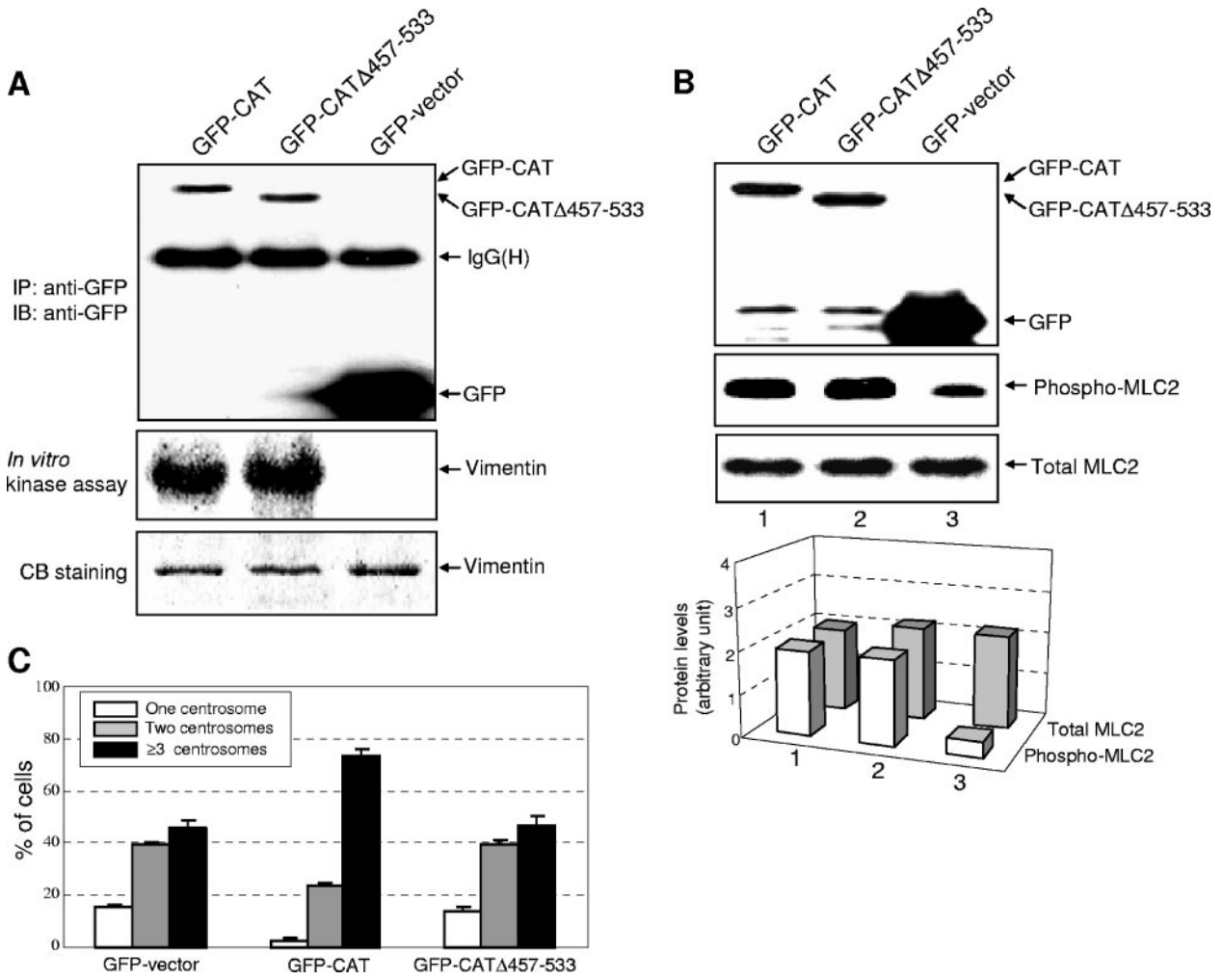

FIG. 5. Centrosomal localization is required for ROCK II to promote centrosome reduplication. (A) NIH 3T3 cells were transfected with GFP-CAT, GFP–CATΔ457-533, or a GFP vector. The lysates were prepared from the transfectants at 18 h after transfection and immunoprecipitated with anti-GFP antibody. The immunoprecipitates were immunoblotted with anti-GFP antibody (top). The immunoprecipitates were also subjected to in vitro kinase assay using vimentin as a substrate as described previously (20) (middle). The substrate band in the Coomassie blue (CB) stain of the gel is shown in the bottom panel. IP, immunoprecipitation; IB, immunoblotting. (B) NIH 3T3 cells were transfected with GFP-CAT, GFP-CATΔ457-533, or a vector control. The lysates prepared at 24 h after transfection were immunoblotted with anti-GFP (top), anti-Ser^{19} phospho-MLC2 (middle), and anti-MLC2 (bottom) antibodies. Quantification of the levels of total and Ser^{19} phospho-MLC2 are shown in the graph at the bottom. (C) NIH 3T3 cells prearrested with Aph for 24 h were transfected with GFP-CAT, GFP–CATΔ457-533, or a GFP vector in the presence of Aph. The transfected cells were incubated for 36 h after transfection in the presence of Aph and immunostained for γ-tubulin, and the centrosome profiles of the GFP-positive cells were analyzed (>300 cells). The results are shown as averages ± standard errors from three independent experiments.

inhibited, suggesting that ROCK II may be dispensable for centrosome duplication per se, but it may be necessary for the efficient initiation of centrosome duplication. Such a function is essential for the coordinated initiation of centrosome duplication and DNA replication. We thus tested whether ROCK II is involved in the timely initiation of centrosome duplication during the cell cycle. For this experiment, we used primary MSFs prepared from adult male mice, since initiation of centrosome duplication and S-phase entry occur in a highly coordinated fashion in these cells. We generated MSFs whose ROCK II expression was silenced by the stable expression of siRNA specific for ROCK II (Fig.6Ca). The control MSFs (transfected with an siRNA vector with a randomized sequence) and ROCK II-RNAi MSFs were synchronized by serum starvation, followed by serum stimulation. Every 3 h for a period of 21 h, cells were examined for progression into S-phase by BrdU incorporation and centrosome duplication by immunostaining with anticentrin antibody (Fig.6Cb; an example of anticentrin antibody immunostaining to detect unduplicated and duplicated centrosomes is shown on the left). Among serum-starved quiescent MSFs, 5 to 8% of cells contain already-duplicated centrosomes. Since centrosomes do not duplicate in the quiescent state, the cells with duplicated centrosomes are likely the ones which were in mid- to late G_1 phase and had duplicated centrosomes but failed to proceed through the cell cycle due to serum deprivation (43). The cell cycle progression through G_1 to S was not altered by the down-regulation of ROCK II: similar BrdU incorporation

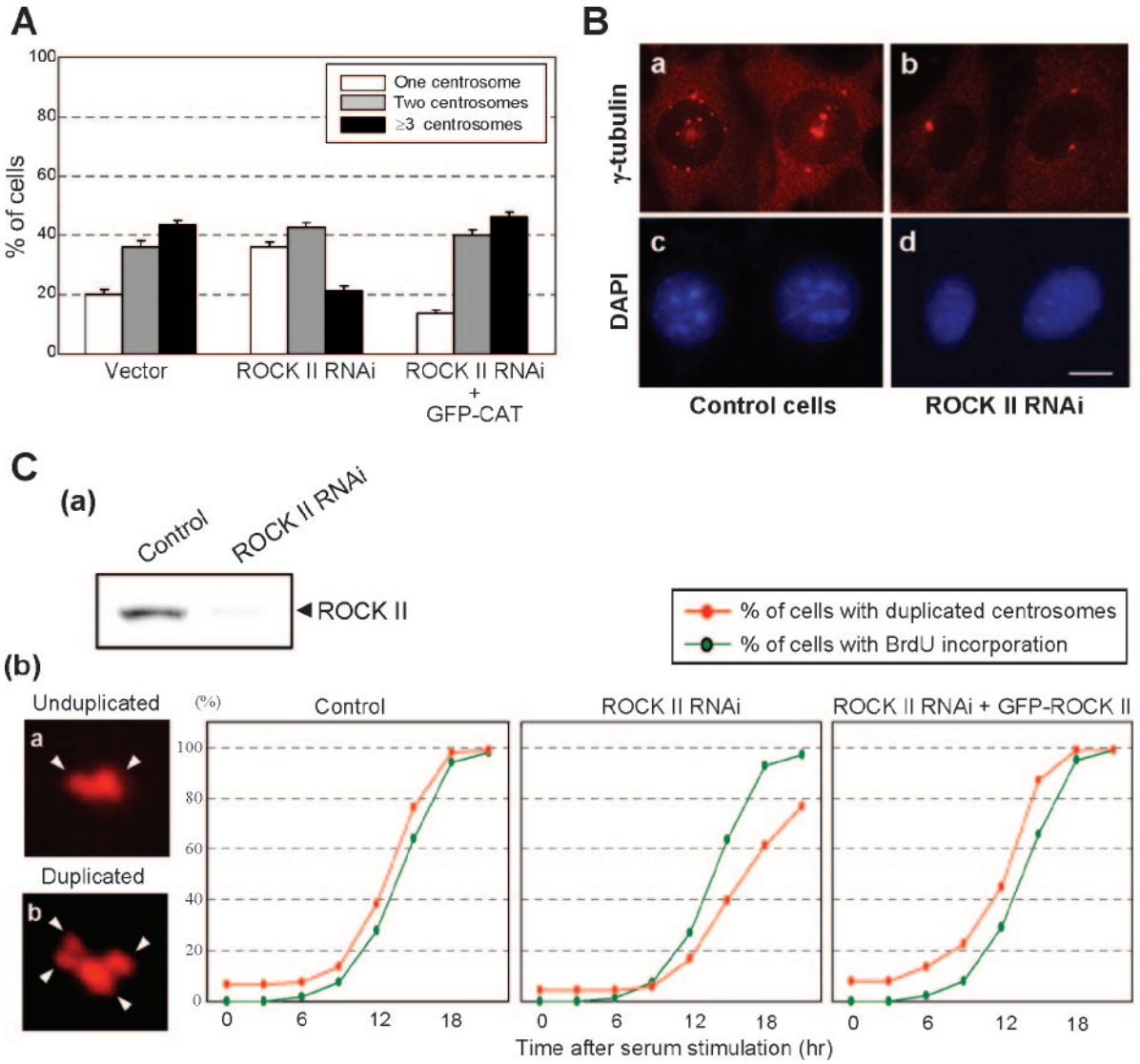

FIG. 6. Role of ROCK II in the timely initiation of centrosome duplication. (A) ROCK II-RNAi and control cells as well as ROCK II-RNAi cells transiently transfected with GFP-CAT were subjected to centrosome reduplication assay. The cells were exposed to Aph for 60 h, and the centrosome profiles were determined by γ-tubulin immunostaining (>300 cells). The results are averages ± standard errors from three experiments. (B) Representative γ-tubulin-immunostained images of the vector control cells and ROCK II-RNAi cells after Aph treatment are shown. Scale bar, 10 μm. (C) MSFs were prepared from the abdominal skin of 8-week-old male mice. MSFs silenced for ROCK II expression and control MSFs were generated by the method used for the generation of NIH 3T3 ROCK II-RNAi cells and control NIH 3T3 cells described in the legend to Fig. 2. (a) Immunoblot analysis of ROCK II expression in ROCK II-RNAi cells and control MSFs. ROCK II-RNAi and control MSFs were serum starved for 30 h and serum stimulated in the presence of BrdU for 21 h. To determine the rates of centrosome duplication and BrdU incorporation, we carried out the experiment with a single cell culture as well as separately with duplicate cultures, which gave almost identical results. For a determination of centrosome duplication, antibody against centrin, a known centriole marker (36), was used. An example of the immunostained images for which anticentrin antibody was used to differentiate unduplicated and duplicated centrosomes is shown on the left. We repeated the experiment twice, and we obtained almost identical results. The averages from two experiments are plotted in the graph.

rates were observed between the ROCK II-RNAi and control cells. In the control cells, the initiation of centrosome duplication and S-phase entry occur in a highly coordinated manner. In contrast, in the ROCK II-RNAi cells, the initiation of centrosome duplication was delayed significantly relative to that of S-phase entry. Moreover, reintroduction of ROCK II, which was engineered to be resistant to the siRNA, into ROCK II-RNAi cells restored the coordinated initiation of centrosome duplication and DNA replication. These observations indicate that ROCK II plays a critical role in the timely initiation of centrosome duplication (and thus the coupling of the initiation of centrosome duplication and DNA replication).

Superactivation of ROCK II by NPM/B23. We next analyzed the functional interaction between ROCK II and NPM/B23. Since the kinase activity is essential for ROCK II to promote centrosome duplication, we tested whether NPM/B23 binding modulates the kinase activity of ROCK II. To this end, baculovirally purified GST–full-length ROCK II and GST-CAT

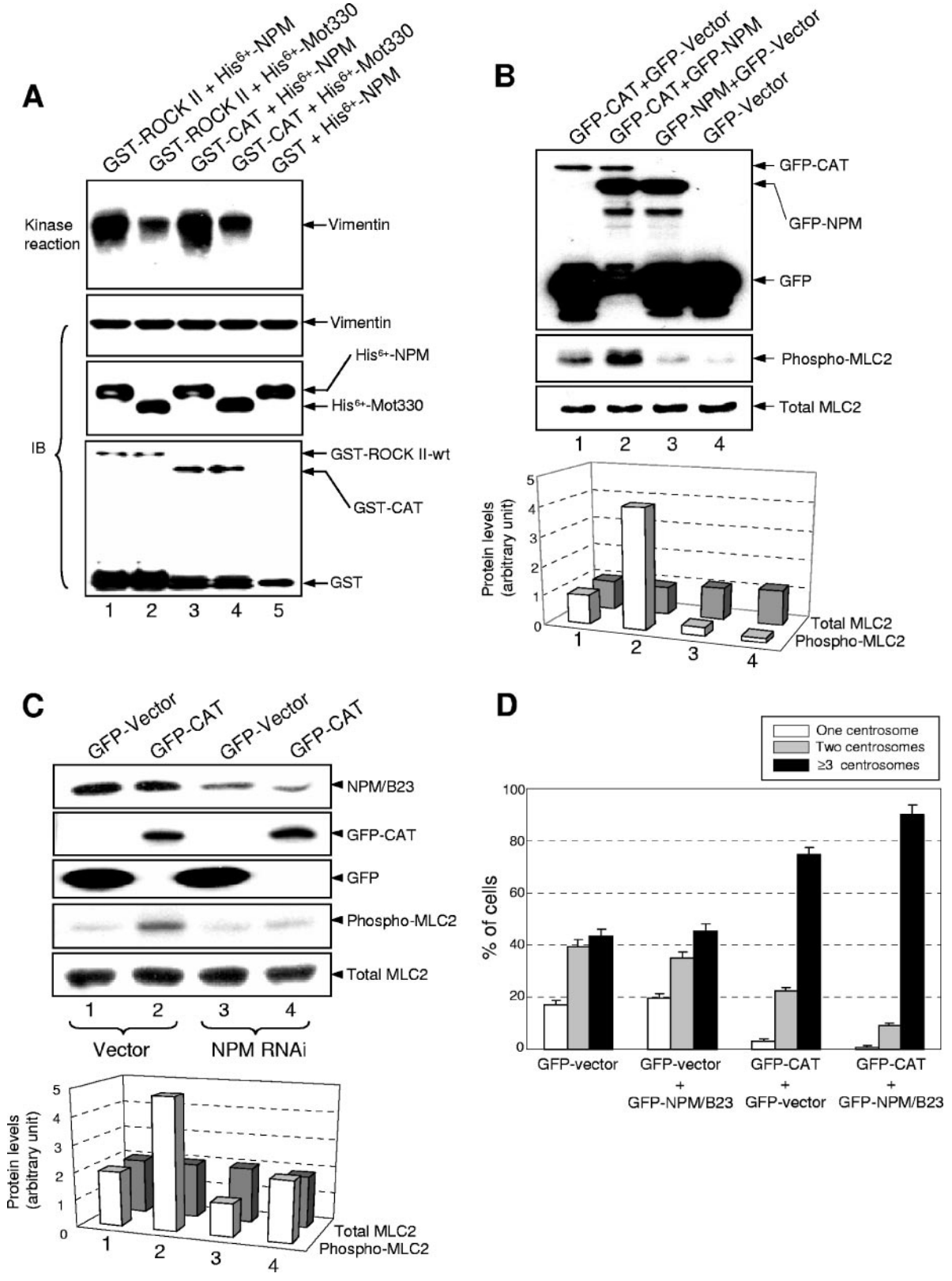

FIG. 7. Superactivation of ROCK II by NPM/B23 in vitro and in vivo and the functional interaction of ROCK II and NPM/B23 to promote centrosome reduplication. (A) Baculovirally prepared GST-CAT and GST-ROCK II were subjected to in vitro kinase assay either in the absence or in the presence of bacterially purified His_6^+-NPM/B23 (top) using vimentin as a substrate. His_6^+-tagged mortalin (Mot330) bacterially prepared by exactly the same method was used as a negative control. GST was also tested as a control. The bottom three panels show the immunoblots (IB) of the kinase reaction samples with antivimentin (second panel), anti-His_6^+ (third panel), and anti-GST (fourth panel) antibodies. wt, wild type.

mutant were subjected to an in vitro kinase assay in either the presence or the absence of His_6^+-NPM/B23 using vimentin as a substrate (Fig. 7A). The His_6^+-tagged partial sequence of mortalin (His_6^+-Mot330) (25), which does not interact with ROCK II or vimentin, was used as a negative control. Although baculovirally purified GST-ROCK II (as well as GST-CAT) is already active because of Rho proteins present in the insect cells (see the results of control reactions with His_6^+-Mot330 in Fig. 7A, lanes 2 and 4), the addition of NPM/B23 markedly increased (more than threefold) the kinase activities of both GST-ROCK II and GST-CAT (lanes 1 and 3). Since NPM/B23 binds to both GST-ROCK II and GST-CAT (Fig. 1), these results strongly suggest that NPM/B23 superactivates ROCK II through direct binding.

To test the NPM/B23-mediated superactivation of ROCK II in vivo, we cotransfected GFP-CAT and GFP-NPM/B23 into cells. For the controls, cells were transfected with GFP-CAT, GFP-NPM/B23, or the GFP vector. Immunoblot analysis with anti-GFP antibody confirmed that comparable levels of GFP-CAT and GFP-NPM/B23 were expressed (Fig. 7B, top). All the transfectants expressed similar levels of total MLC2 (Fig. 7B, bottom), while the level of Ser^{19}-phosphorylated MLC2 was increased in the GFP-CAT-transfected cells (Fig. 7B, middle, lane 1) compared with that in the control vector-transfected cells (lane 4). However, the cotransfection of GFP-NPM/B23 further increased the level of phospho-Ser^{19} MLC2 (Fig. 7B, middle, lane 2). Thus, as occurs in vitro, NPM/B23 superactivates ROCK II in vivo.

To examine the physiological significance of the superactivation of ROCK II by NPM/B23, we first attempted to silence NPM/B23 by siRNA. However, NPM/B23 is essential for cell survival, and we could only partially silence the expression of NPM/B23 to ~30% of the normal level (Fig. 7C, top, lanes 3 and 4), which is consistent with the recent studies that attempted to generate NPM/B23-deficient mice (15). Nevertheless, we examined whether partial silencing of NPM/B23 expression affects ROCK II activity. NPM/B23 RNAi cells and control cells (transfected with an siRNA vector containing randomized sequence) were transfected with either GFP-CAT or the GFP vector. Similar levels of GFP-CAT (Fig. 7C, second panel) and GFP (third panel) were expressed in the NPM/B23 RNAi and control cells. The levels of total MLC2 were comparable among all the transfectants (Fig. 7C, fifth panel), while the level of Ser^{19}-phosphorylated MLC2 was increased in the GFP-CAT-transfected control cells (fourth panel, lane 2) compared with that in the control GFP vector-transfected cells (lane 1). However, in the NPM RNAi cells, GFP-CAT expression only minimally increased the level of phospho-Ser^{19} MLC2 (Fig. 7C, fourth panel, lane 4). These findings further demonstrate that NPM/B23 and ROCK II functionally interact in vivo.

NPM/B23 has been shown to localize between the paired centrioles within the centrosome proper and is likely involved in the pairing of centrioles (38). Since separation of the paired centrioles is the initial event of centrosome duplication, NPM/B23 acts as a negative regulator of centrosome duplication in this context. However, the findings that ROCK II promotes centrosome duplication and NPM/B23 superactivates ROCK II lead us to predict that NPM/B23 may also participate in the regulation of centrosome duplication in a positive manner via ROCK II. To test this possibility, we cotransfected GFP-CAT and GFP-NPM/B23 into NIH 3T3 cells prearrested by Aph. As a control, the GFP vector was transfected alone or with either GFP-CAT or GFP-NPM/B23. After transfection, cells continued to be exposed to Aph for 36 h, and the centrosome profiles of the GFP-positive cells were determined (Fig. 7D). The expression of GFP-NPM/B23 alone did not significantly alter the frequency of centrosome reduplication significantly. As shown earlier, GFP-CAT expression accelerated centrosome reduplication in NIH 3T3 cell (~75%). However, the cotransfection of NPM/B23 further accelerated centrosome reduplication (>90%), demonstrating the functional interaction between NPM/B23 and ROCK II to promote centrosome reduplication.

Thr^{199} phosphorylation is important for NPM/B23 to superactivate ROCK II in vivo. CDK2/cyclin E phosphorylates NPM/B23 on Thr^{199}, and this phosphorylation is critical for the initiation of centrosome duplication (46). We next tested whether the Thr^{199} phosphorylation of NPM/B23 plays a role in the superactivation of the ROCK II and ROCK II-dependent promotion of centrosome duplication using the phosphomimetic mutant NPM/B23. For this particular experiment, the standard centrosome reduplication assay may not be appropriate, since cotransfection of wild-type NPM/B23 and CAT induces centrosome reduplication in > 90% of cells (Fig. 7D); hence, further acceleration of centrosome duplication cannot be confidently determined. To circumvent this problem, we decided to shorten the duration of Aph exposure after transfection. In the standard centrosome reduplication assay, cells were exposed to Aph for total 72 h (24 h of prearresting plus 12 h of transfection plus 36 h of incubation). In this experiment, the final incubation time was shortened to 18 h. FLAG epitope-tagged wild-type NPM/B23, the T199A mutant (un-

(B) Cells were transfected with GFP-CAT plus the GFP vector, GFP-CAT plus GFP-NPM/B23, GFP-NPM/B23 plus the GFP vector, or the GFP vector alone. The lysates were prepared at 24 h posttransfection and immunoblotted with anti-GFP antibody (top), anti-phospho-Ser^{19} MLC2 antibody (middle), and anti-MLC2 antibody (bottom). The quantifications of the levels of total and phospho-Ser^{19} MLC2 are shown in the graph. (C) Either a pSuper plasmid encoding the RNAi sequence targeted for NPM/B23 or a control plasmid with a randomized sequence with the same nucleotide composition was cotransfected with a plasmid encoding a puromycin resistance gene as a rapid selection marker into NIH 3T3 cells. After 3 days of puromycin selection, the drug-resistant cells were pooled and transfected with GFP-CAT. The lysates were prepared from the transfectants at 24 h posttransfection and subjected to immunoblot analysis using anti-NPM/B23 (first panel), anti-GFP (second and third panels), anti-phospho-Ser^{19} MLC2 (fourth panel), and anti-MLC2 (fifth panel) antibodies. Quantifications of the levels of total and phospho-Ser^{19} MLC2 are shown in the graph. (D) NIH 3T3 cells prearrested by Aph treatment for 24 h were transfected with GFP-NPM/B23 plus the GFP vector, GFP-CAT plus the GFP vector, GFP-CAT plus GFP-NPM/B23, or the GFP vector alone. After transfection, cells were exposed to Aph for 36 h, and the centrosome profiles of the GFP-positive cells were determined (>300 cells). The results shown are averages ± standard errors from three independent experiments.

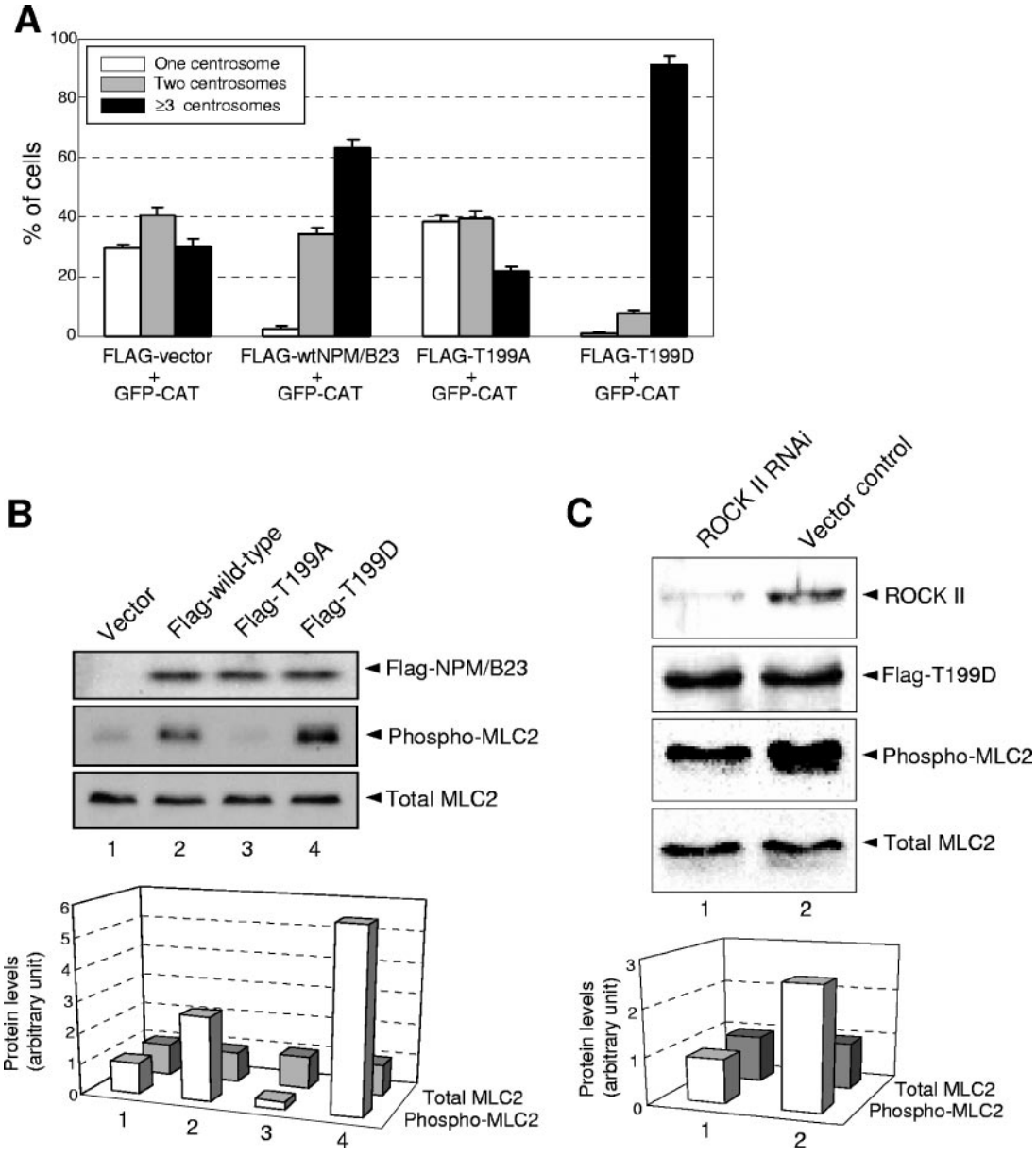

FIG. 8. Thr[199] phosphorylation is important for NPM/B23 to superactivate ROCK II and to enhance the activity of ROCK II to promote centrosome reduplication. (A) NIH 3T3 cells prearrested by Aph treatment for 24 h were cotransfected with FLAG-tagged wild-type (wt) NPM/B23, the T199A mutant, the T199D mutant, or a vector control with GFP-CAT. After transfection, cells were incubated in the presence of Aph for 18 h, and the centrosome profiles of the GFP-positive cells were determined (>200 cells). The results shown are averages ± standard errors from three independent experiments. (B) NIH 3T3 cells were transfected with FLAG-tagged wild-type NPM/B23, the FLAG-tagged T199A mutant, the FLAG-tagged T199D mutant, or a vector plasmid. The lysates were prepared at 36 h posttransfection and immunoblotted with anti-FLAG (top blot), anti-phospho-Ser[19] MLC2 (middle blot), and anti-MLC2 antibodies (bottom blot). Quantification of the levels of total and phospho-Ser[19] MLC2 are shown in the graph at the bottom. (C) ROCK II-RNAi cells (NIH 3T3 origin) and the vector control cells were transfected with the FLAG-tagged T199D mutant. The lysates were prepared at 24 h posttransfection and immunoblotted with anti-ROCK II (first blot), anti-FLAG (second blot), anti-phospho-Ser[19] MLC2 (third blot), and anti-MLC2 (fourth blot) antibodies. Quantifications of the levels of total and phospho-Ser[19] MLC2 are shown in the graph at the bottom.

phosphorylatable mutant NPM/B23; Thr[199]→Ala), the T199D mutant (phospho-mimetic mutant NPM/B23; Thr[199]→Asp), or a control vector was cotransfected with GFP-CAT into NIH 3T3 cells prearrested with Aph. After transfection, cells were exposed to Aph, and the centrosome profiles of the GFP-positive cells were determined (Fig. 8A). Under this protocol, the expression of GFP-CAT resulted in a frequency of centrosome reduplication of ~30%, and the cotransfection of wild-type NPM/B23 and GFP-CAT resulted in the further induction of centrosome amplification to ~60%. The cotransfection of the NPM/B23 T199A mutant and GFP-CAT resulted in a minimal induction of centrosome amplification (~20%) at least in part due to the negative regulatory activity resulting from the T199A mutation of centrosome duplication, as shown

previously (46). In contrast, the cotransfection of the T199D mutant and GFP-CAT resulted in a marked increase in the frequency of centrosome amplification (>90%), indicating that Thr^{199}-phosphorylated NPM/B23 further enhances ROCK II activity to promote centrosome reduplication.

We next tested the potential changes in ROCK II kinase activity in vivo by expressing the T199A and T199D NPM/B23 mutants. NIH 3T3 cells were transfected with a control vector, FLAG-tagged wild-type NPM/B23, or the T199A or T199D NPM/B23 mutant and examined for levels of Ser^{19} phosphorylation of MLC2 by immunoblot analysis (Fig. 8B). Similar levels of the FLAG-T199A mutant, the T199D mutant, and wild-type NPM/B23 were expressed (Fig. 8B, top blot). There was an approximately twofold increase in the level of phospho-Ser^{19} MLC2 in the wild-type NPM/B23 transfectants (Fig. 8B, middle blot, lane 2) compared with the level in the control cells (lane 1), However, the level of phospho-Ser^{19} MLC2 was further increased (approximately fivefold) in the T199D transfectants (lane 4), while there was a noticeable decrease in the level of phospho-Ser^{19} MLC2 in the T199A transfectants (lane 3). Thus, phosphorylation on Thr^{199} plays a role in the NPM/B23-mediated superactivation of ROCK II in vivo, while the expression of a nonphosphorylatable mutant may act in a dominant negative manner. To exclude the possibility that the T199D mutant may affect a kinase(s) other than ROCK II, resulting in an increase in phospho-Ser^{19} MLC2, we transfected the FLAG-T199D mutant into ROCK II-RNAi and control cells. The lysates from both transfectants were subjected to immunoblot analysis (Fig. 8C). Both transfectants expressed similar levels of the T199D mutant (Fig. 8C, second blot). The level of Ser^{19} phospho-MLC2 was up-regulated by the expression of the T199D mutant in the control cells (Fig. 8C, third blot, lane 2) but not in the ROCK II-RNAi cells (lane 1). Thus, the increase in the phospho-Ser^{19} MLC2 level is due to the enhanced kinase activity of ROCK II by the T199D mutant.

Cell cycle-dependent interaction between NPM/B23 and ROCK II. Since NPM/B23 superactivates ROCK II through direct physical interaction, we tested whether Thr^{199} phosphorylation affects NPM/B23's ability to bind to ROCK II. NIH 3T3 cells were transfected with either the FLAG-tagged T199A mutant or the T199D mutant, and the transfectants were subjected to coimmunoprecipitation assay using anti-FLAG and anti-ROCK II antibodies (Fig. 9A). Anti-ROCK II antibody coimmunoprecipitated approximately threefold more of the T199D mutant proteins than of the T199A mutant proteins (Fig.9Aa). Similarly, anti-FLAG antibody coimmunoprecipitated approximately threefold more ROCK II in the T199D mutant-transfected cells than the T199A mutant-transfected cells (Fig.9Ab), indicating that Thr^{199} phosphorylation enhances the ROCK II binding affinity of NPM/B23.

We next performed an in vitro kinase assay using baculovirally prepared GST-ROCK II in the presence of either the His_6^+-tagged T199A mutant or the T199D mutant in various concentrations, with vimentin as a substrate (Fig. 9B). At higher concentrations, both the T199A and the T199D mutant equally superactivated ROCK II. However, at lower concentrations, only the T199D transfectant could efficiently superactivate ROCK II, further demonstrating that Thr^{199} phosphorylation increases the ROCK II binding affinity of NPM/B23 and thus allows more-efficient superactivation of ROCK II.

The ability of a minimal concentration of Thr^{199}-phosphorylated NPM/B23 to superactivate ROCK II may be critical in vivo, where the quantities of proteins are limited, raising the possibility that only NPM/B23 phosphorylated on Thr^{199} may form a complex with ROCK II in vivo. To test this possibility, NIH 3T3 cells were serum starved for 24 h and serum stimulated. At every 3 h for a period of 18 h, cells were harvested and examined for CDK2/cyclin E activity and ROCK II-NPM/B23 complex formation (Fig. 9C). The in vitro histone H1 kinase assay of immunoprecipitated CDK2/cyclin E showed the expected kinetics of CDK2/cyclin E activation during G_1 progression (Fig. 9C, first panel). There was no significant change in the levels of NPM/B23 and ROCK II during the cell cycle progression (Fig, 9C, second and third panels, respectively). As described previously (32, 46), NPM/B23 phosphorylated on Thr^{199} gradually accumulates during the G_1 progression in association with CDK2/cyclin E activation (Fig. 9C, fourth panel). The lysates were also immunoprecipitated with anti-ROCK II antibody, and the immunoprecipitates were immunoblotted with either anti-NPM/B23 (Fig. 9C, fifth panel) or anti-phospho-Thr^{199} NPM/B23 (sixth panel) antibodies. We found that complex formation between ROCK II and NPM/B23 becomes evident in mid- to late G_1, and the kinetics of ROCK II-NPM/B23 complex formation parallels those of CDK2/cyclin E activation and the emergence of phospho-Thr^{199} NPM/B23. These observations strongly suggest that complex formation between ROCK II and NPM/B23 in vivo depends on the Thr^{199} phosphorylation of NPM/B23.

The interaction between NPM/B23 and ROCK II at centrosomes is required for the ROCK II-dependent promotion of centrosome duplication. To test whether interaction between ROCK II and NPM/B23 needs to occur at centrosomes for ROCK II to promote centrosome duplication, we decided to use the NPM/B23 missense mutant that can no longer localize to centrosomes. We have identified Lys^{263} of NPM/B23 as a critical residue for NPM/B23 to localize to centrosomes. For instance, the NPM/B23 K263R missense mutant (Lys^{263}→Arg) fails to localize to centrosomes (unpublished data). We first examined whether the K263R mutant retains the ability to interact with ROCK II. FLAG-tagged wild-type NPM/B23 and the K263R mutant were transfected into NIH 3T3 cells. As a control, a vector plasmid was transfected. The lysates prepared from the transfectants were subjected to coimmunoprecipitation assay using anti-ROCK II and anti-FLAG antibodies (Fig. 10A). Similar levels of ROCK II were coimmunoprecipitated with FLAG–wild-type NPM/B23 and the K263R mutant (Fig. 10A, second panel), and similar levels of FLAG–wild-type NPM/B23 and the K263R mutant were coimmunoprecipitated with ROCK II (fourth panel). Thus, the K263R mutant binds to ROCK II as efficiently as wild-type NPM/B23.

We next tested whether the K263R mutant retains the ability to superactivate ROCK II. Bacterially purified His_6^+-tagged wild-type and mutant NPM/B23 proteins (the T199D mutant, the K263R mutant, and the T199D/K263R double mutant) were tested for their activities in superactivating GST-CAT in vitro (Fig. 10B). As with the results shown in Fig. 9B, wild-type NPM/B23 (unphosphorylated NPM/B23) superactivated GST-CAT in a concentration-dependent manner (Fig. 10B, lanes 2 and 3),

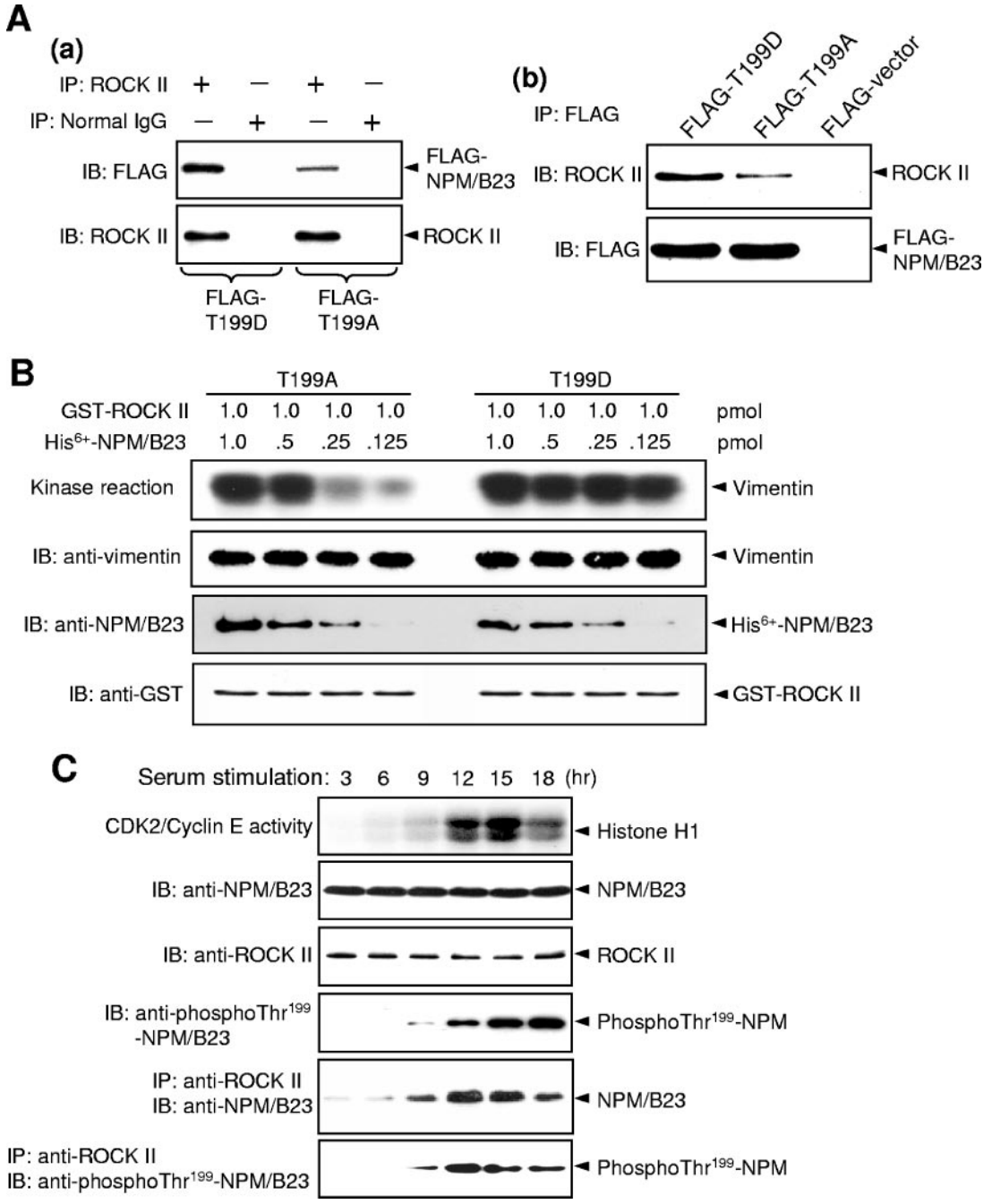

FIG. 9. Thr^{199} phosphorylation of NPM/B23 is critical for NPM/B23-ROCK II complex formation in vivo. (A) NIH 3T3 cells were transfected with either the FLAG-tagged T199D mutant or the FLAG-tagged T199A mutant. The lysates were prepared at 24 h posttransfection and subjected to immunoprecipitation (IP) with either anti-ROCK II (a) or anti-FLAG (b) antibodies. The immunoprecipitates were then immunoblotted (IB) with anti-FLAG and anti-ROCK II antibodies. (B) Baculovirally purified GST-ROCK II was subjected to in vitro kinase assay in the presence of various concentrations of either the His_6^+-tagged T199A mutant or the His_6^+-tagged T199D mutant with vimentin as a substrate (top panel). Aliquots of the kinase reaction mixtures were immunoblotted with antivimentin, anti-NPM/B23, and anti-GST antibodies. We also tested GST-CAT, and we obtained similar results (data not shown). (C) NIH 3T3 cells were serum starved for 24 h and serum stimulated. Every 3 h for a period of 18 h, lysates were prepared. The lysates were immunoprecipitated with anti-cyclin E antibody, and the immunoprecipitates were subjected to in vitro histone H1 kinase assay (first panel). The lysates were also immunoblotted with anti-NPM/B23 (second panel), anti-ROCK II (third panel), and anti-phospho-Thr^{199} NPM/B23 (fourth panel) antibodies. The lysates were also immunoprecipitated with anti-ROCK II antibody, and the immunoprecipitates were immunoblotted with anti-NPM/B23 antibodies (fifth panel) as well as anti-phospho-Thr^{199} NPM/B23 antibodies (bottom panel).

while both high and low concentrations of the T199D mutant superactivated GST-CAT (lanes 4 and 5). The K263R mutant superactivated GST-CAT in a concentration-dependent manner (Fig. 10B, lanes 6 and 7), similar to what occurred with wild-type NPM/B23, while both high and low concentrations of the T199D K283R double mutant superactivated GST-CAT (lanes 8 and 9). Thus, the K263R mutant retains full activity to superactivate ROCK II, and its activity is influenced by phosphorylation on Thr^{199}.

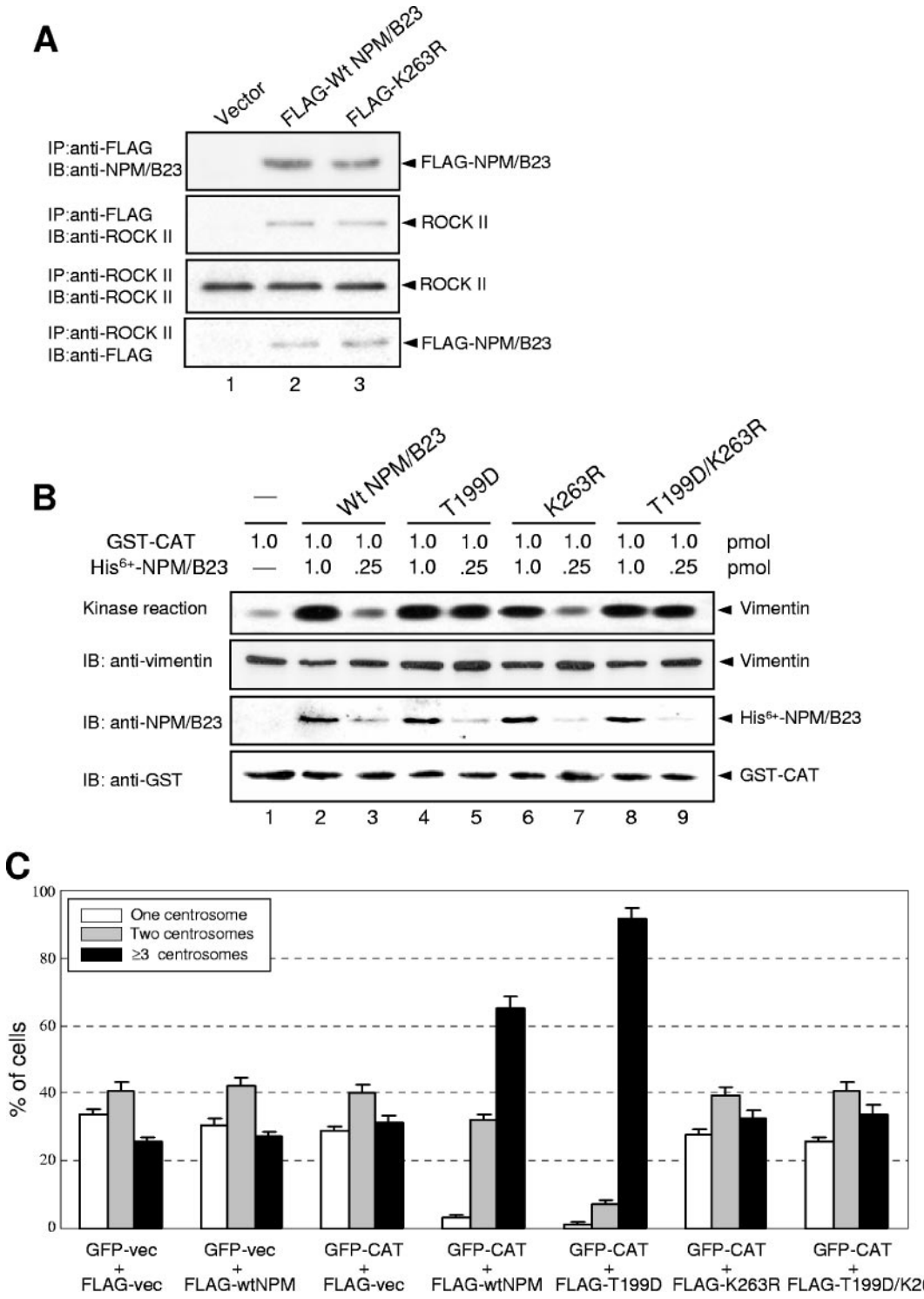

FIG. 10. Centrosome localization is critical for NPM/B23 to augment ROCK II activity to promote centrosome reduplication. (A) NIH 3T3 cells were transfected with FLAG-tagged wild-type (Wt) NPM/B23, the K263R mutant, or a vector plasmid. At 24 h posttransfection, the lysates were prepared and subjected to immunoprecipitation (IP) using either anti-FLAG or anti-ROCK II antibody. The immunoprecipitates were then immunoblotted (IB) with ant-FLAG as well as anti-ROCK II antibodies. (B) Baculovirally purified GST-CAT was subjected to in vitro kinase assay in the presence of His_6^+-tagged wild-type NPM/B23, the T199D mutant, the K263R mutant, or the T199D K263R mutant at two different concentrations with vimentin as a substrate (first panel). Aliquots of the kinase reaction mixtures were immunoblotted with antivimentin, anti-NPM/B23, and anti-GST antibodies. We also tested GST–full-length ROCK II, and we obtained similar results (data not shown). (C) NIH 3T3 cells prearrested by Aph treatment for 24 h were cotransfected with GFP-CAT plus FLAG-tagged wild-type NPM/B23, GFP-CAT plus the T199D mutant, GFP-CAT plus the K263R mutant, or GFP-CAT plus the T199D/K263R mutant. For controls, cells were cotransfected with the GFP vector (GFP-vec) plus the FLAG vector (FLAG-vec), the GFP vector plus FLAG-tagged wild-type NPM/B23, or GFP-CAT plus the FLAG vector. After transfection, cells were incubated in the presence of Aph for 18 h, and the centrosome profiles of the GFP-positive cells were determined (>200 cells). The results shown are averages ± standard errors from three independent experiments.

We then tested the K263R mutant for its ability to aid ROCK II to promote centrosome duplication by centrosome reduplication assay. Since we also tested the T199D K263R double mutant, the modified centrosome reduplication assay (18 h of Aph exposure after transfection) described for Fig. 8A was used. We cotransfected GFP-CAT with FLAG-tagged wild-type NPM/B23 and the T199D, K263R, or T199D/K263R mutant into NIH 3T3 cells prearrested with Aph. After transfection, cells were further exposed to Aph for 18 h, and the centrosome profiles of the GFP-positive cells were determined (Fig. 10C). As shown in Fig. 8A, wild-type NPM/B23 augmented the ROCK II-mediated promotion of centrosome reduplication (~60%), and the T199D phospho-mimetic mutant did so more efficiently (>90%). However, both the K263R and T199D/K263R mutants failed to augment the activity of GFP-CAT to promote centrosome reduplication; the frequency of centrosome amplification was similar to that of the vector-transfected control cells (~30%). Thus, NPM/B23 requires centrosome localization to augment ROCK II to promote centrosome duplication, implying that NPM/B23 and ROCK II need to interact with each other at centrosomes to promote centrosome duplication.

DISCUSSION

In this study, we identified ROCK II as a centrosomal protein that interacts with NPM/B23 with a high affinity. We further found that ROCK II promotes centrosome duplication in its kinase and centrosome localization-dependent manner. In cells in which ROCK II expression is silenced, the initiation of centrosome duplication, which normally occurs at late G_1/early S phase, was significantly delayed, although centrosomes were eventually duplicated prior to mitosis. Thus, ROCK II may be dispensable for centrosome duplication per se but required for the timely initiation of centrosome duplication, and thus the initiation of centrosome duplication and S-phase entry are coupled. We further found that NPM/B23 superactivates ROCK II by physical interaction, and this interaction is enhanced by the Thr^{199} phosphorylation of NPM/B23. For instance, NPM/B23 with a phospho-mimetic mutation at Thr^{199} shows a significantly higher binding affinity for ROCK II than unphosphorylated NPM/B23. Moreover, the phospho-mimetic NPM/B23 mutant superactivates ROCK II with a minimal concentration. Since the quantities of specific proteins are limited in cells, the acquisition of a higher affinity of binding to the partner proteins by posttranslational modifications (e.g., phosphorylation) becomes a critical event. Indeed, the complex formation of NPM/B23 and ROCK II is cell cycle dependent and occurs in association with the activation of CDK2/cyclin E and the emergence of phospho-Thr^{199} NPM/B23. Thus, the ROCK II binding of NPM/B23 and consequential superactivation of ROCK II in vivo is likely controlled by phosphorylation on Thr^{199} mediated by CDK2/cyclin E. Since the centrosome-binding mutant NPM/B23 can no longer augment the activity of ROCK II to promote centrosome duplication, interaction between ROCK II and NPM/B23 must occur at centrosomes to promote centrosome duplication. All these findings converge to model the molecular events associated with the initiation of centrosome duplication (Fig. 11). At late G_1, CDK2/cyclin E is activated by the temporal expression of cyclin E, which phosphorylates NPM/B23 on Thr^{199} at centrosomes. Thr^{199} phosphorylation triggers the majority of NPM/B23 proteins to dissociate from centrosomes, but some NPM/B23 proteins remain at centrosomes. Indeed, we could readily detect NPM/B23 phosphorylated on Thr^{199} in the centrosomes isolated from cells exposed to Aph for 36 h (>80% of cells after 36 h of Aph exposure contain duplicated centrosomes), and NPM/B23 phosphorylated on Thr^{199} could be detected immunocytochemically on one of the duplicated centrosomes, presumably the one with the mother centriole of the

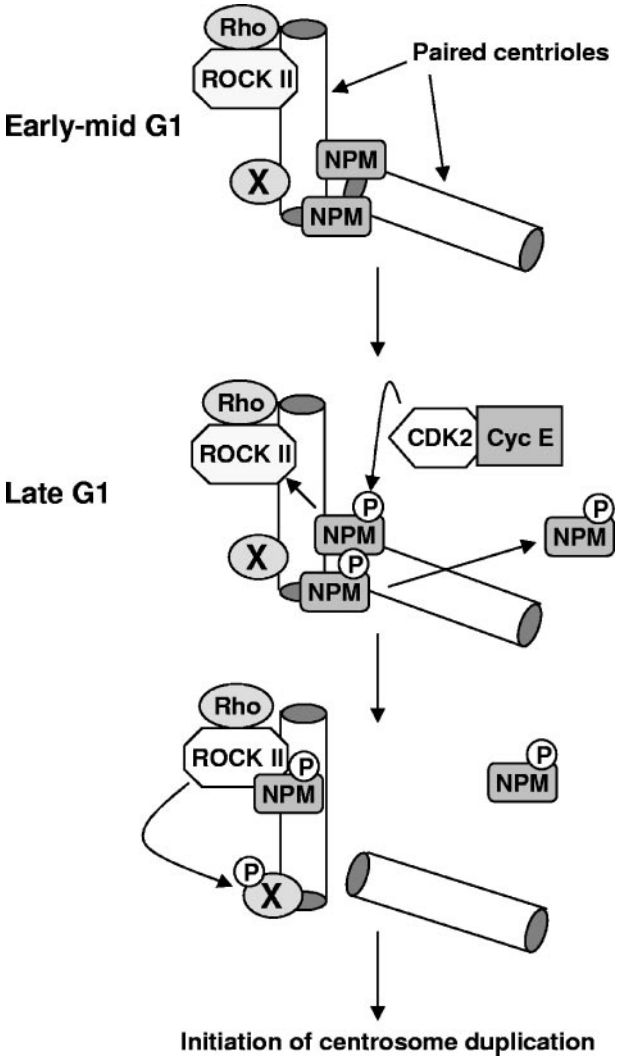

FIG. 11. Model of the ROCK II-NPM/B23-mediated regulation of centrosome duplication. During the early to mid-G_1 phase of the cell cycle, NPM/B23 localizes between the paired centrioles of unduplicated centrosomes, likely functioning in pairing the centrioles. In late G_1, CDK2/cyclin E becomes activated and phosphorylates NPM/B23 on Thr^{199}. Upon Thr^{199} phosphorylation, the majority of NPM/B23 proteins dissociate from centrosomes, but some remain at centrosomes and translocate toward the mother centriole of the pair. These Thr^{199}-phosphorylated NPM/B23 proteins have high binding affinities to ROCK II and bind to ROCK II present at centrosomes. ROCK II is superactivated by NPM/B23 binding and rapidly targets the protein (shown as "X") which plays a key role in the initiation of centrosome duplication.

original pair, based on our previous findings (38; Z. Ma, unpublished observation). Upon Thr^{199} phosphorylation, NPM/B23 acquires a high binding affinity for ROCK II and interacts with ROCK II, which in turn superactivates ROCK II. ROCK II then rapidly and efficiently targets the key centrosomal protein(s) for initiation of centrosome duplication. Although the identification of such a target protein(s) is under way in our laboratory, we predict that it likely functions in the splitting of the paired centrioles, an initial event of centrosome duplication, for the following reasons. Within the unduplicated centrosome, NPM/B23 localizes between the paired centrioles (38). In late G_1, the majority of NPM/B23 proteins dissociate from centrosomes upon CDK2/cyclin E-mediated phosphorylation on Thr^{199}. However, some NPM/B23 proteins remain at centrosomes, and they move toward the mother centriole of the pair prior to centriole splitting (38). Thus, after centriole splitting, only the mother centriole is bound by NPM/B23, which makes it highly unlikely that the ROCK II-NPM/B23 complex functions in procentriole formation. Procentrioles form on both centrioles. Therefore, it is more likely that the ROCK II-NPM/B23 complex formed at mother centrioles upon the phosphorylation of NPM/B23 by CDK2/cyclin E functions in the process of splitting of the paired centrioles. Such a function of the ROCK II-NPM/B23 complex may be critical for the timely initiation of centrosome duplication and the coupling of centrosome duplication and DNA replication.

It has been shown that the majority of ROCK II-null embryos die early in development, yet a small percentage of mice develop normally (45), suggesting that ROCK II deficiency can be inefficiently compensated for by other proteins, perhaps ROCK I, another member of the ROCK kinase family. With respect to the duplication of centrosomes, ROCK II expression-silenced cells eventually duplicate centrosomes despite the delayed initiation of centrosome duplication. At present, we do not know whether centriole splitting occurs eventually without the activity of ROCK II or whether the ROCK II activity is compensated for (inefficiently) by other kinases in cells whose ROCK II expression is silenced. If the latter is the case, ROCK I is the most likely candidate. It has been shown that ROCK I also localizes to centrosomes and is involved in the proper pairing and positioning of centrioles: the down-regulation of ROCK I results in the erratic motion of mother centrioles during G_1 and premature centriole migration in the midbody during mitosis (8). ROCK I and ROCK II have been shown to share many substrates, although they target the substrate with different efficiencies (50). Although NPM/B23 does not bind to ROCK I, ROCK I, like ROCK II, is already active by binding to Rho but not superactivated. Thus, ROCK I may be able to inefficiently compensate for ROCK II, resulting in the eventual initiation of centrosome duplication after a significant delay.

NPM/B23 is involved in diverse biological events and pathways and often simultaneously participates in two functionally opposing events/pathways. For instance, NPM/B23 influences cellular proliferation and transformation both positively (oncogenically) and negatively (antioncogenically). Thus, it is not surprising that NPM/B23 is involved in the regulation of centrosome duplication through multiple functionally opposing pathways. We have previously shown that the unphosphorylatable NPM/B23 T199A mutant acts as a dominant negative when expressed in cells, resulting in the suppression of centrosome duplication (46). NPM/B23 localizes between paired centrioles within the unduplicated centrosome, likely functioning as a glue-like protein for centriole pairing. Upon phosphorylation on Thr^{199}, NPM/B23 either dissociates from centrosomes or shifts its subcentrosomal localization. The T199A mutant can neither dissociate from centrosomes nor shift its subcentrosomal localization even in the presence of active CDK2/cyclin E, resulting in a failure of the paired centrioles to undergo physical separation; hence, centrosome duplication is suppressed. In this context, NPM/B23 negatively controls centrosome duplication, which is released by Thr^{199} phosphorylation by CDK2/cyclin E. Here, we found that NPM/B23 upon phosphorylation on Thr^{199} acquires a high affinity for binding to ROCK II, physically associating with and superactivating ROCK II at centrosomes, which in turn promotes centrosome duplication. Why then do the cells derived from mice whose NPM/B23 expression is depleted to 10 to 30% of the normal level suffer centrosome amplification (15)? If the protein is involved in the regulation of one biological event through multiple pathways, when the expression of the protein is either lost or reduced in mice, it is difficult to predict which pathway will be more affected than the others by loss/depletion of the protein and emerge as a predominant phenotype. Among its multiple functions, the functions which are more readily compensated for by other proteins or mutations will more likely be masked and will not result in abnormal phenotypes. In the case of NPM/B23, with respect to the regulation of centrosome duplication, the positive regulatory function of ROCK II may be more readily compensated for by other proteins or mutations than its negative regulatory function exerted on centriole pairing. Thus, the loss of the negative regulatory function may emerge as a predominant phenotype in mice with reduced NPM/B23 expression.

ACKNOWLEDGMENTS

We thank K. George for technical assistance.

This research is supported by a grant from the National Institutes of Health (CA95925).

REFERENCES

1. **Amano, M., M. Ito, K. Kimura, Y. Fukata, K. Chihara, T. Nakano, Y. Matsuura, and K. Kaibuchi.** 1996. Phosphorylation and activation of myosin by Rho-associated kinase (Rho-kinase). J. Biol. Chem. **271:**20246–20249.
2. **Amano, M., K. Chihara, N. Nakamura, T. Kaneko, Y. Matsuura, and K. Kaibuchi.** 1999. The COOH-terminus of Rho-kinase negatively regulates rho-kinase activity. J. Biol. Chem. **274:**32418–32424.
3. **Balczon, R., L. Bao, W. E. Zimmer, K. Brown, R. P. Zinkowski, and B. R. Brinkley.** 1995. Dissociation of centrosome replication events from cycles of DNA synthesis and mitotic division in hydroxyurea-arrested Chinese hamster ovary cells. J. Cell Biol. **130:**105–115.
4. **Borer, R. A., C. F. Lehner, H. M. Eppenberger, and E. A. Nigg.** 1989. Major nucleolar proteins shuttle between nucleus and cytoplasm. Cell **56:**379–390.
5. **Brady, S. N., Y. Yu, L. B. Maggi, Jr., and J. D. Weber.** 2004. ARF impedes NPM/B23 shuttling in an Mdm2-sensitive tumor suppressor pathway. Mol. Cell. Biol. **24:**9327–9338.
6. **Chen, X. Q., I. Tan, C. H. Ng, C. Hall, L. Lim, and T. Leung.** 2002. Characterization of RhoA-binding kinase ROKalpha implication of the pleckstrin homology domain in ROKalpha function using region-specific antibodies. J. Biol. Chem. **277:**12680–12688.
7. **Chen, Z., V. B. Indjeian, M. McManus, L. Wang, and B. D. Dynlacht.** 2002. CP110, a cell cycle-dependent CDK substrate, regulates centrosome duplication in human cells. Dev. Cell **3:**339–350.
8. **Chevrier, V., M. Piel, N. Collomb, Y. Saoudi, R. Frank, M. Paintrand, S. Narumiya, M. Bornens, and D. Job.** 2002. The Rho-associated protein kinase p160ROCK is required for centrosome positioning. J. Cell Biol. **157:**807–817.

9. **Coleman, M. L., E. A. Sahai, M. Yeo, M. Bosch, A. Dewar, and M. F. Olson.** 2001. Membrane blebbing during apoptosis results from caspase-mediated activation of ROCK I. Nat. Cell Biol. **3:**339–345.
10. **Doxsey, S.** 2001. Re-evaluating centrosome function. Nat. Rev. Mol. Cell. Biol. **2:**688–698.
11. **Feng, J., M. Ito, K. Ichikawa, N. Isaka, M. Nishikawa, D. J. Hartshorne, and T. Nakano.** 1999. Inhibitory phosphorylation site for Rho-associated kinase on smooth muscle myosin phosphatase. J. Biol. Chem. **274:**37385–37390.
12. **Fisk, H. A., and M. Winey.** 2001. The mouse Mps1p-like kinase regulates centrosome duplication. Cell **106:**95–104.
13. **Fukasawa, K.** 2005. Centrosome amplification, chromosome instability and cancer development. Cancer Lett. **230:**6–19.
14. **Goto, H., H. Kosako, K. Tanabe, M. Yanagida, M. Sakurai, M. Amano, K. Kaibuchi, and M. Inagaki.** 1998. Phosphorylation of vimentin by Rho-associated kinase at a unique amino-terminal site that is specifically phosphorylated during cytokinesis. J. Biol. Chem. **273:**11728–11736.
15. **Grisendi, S., R. Bernardi, M. Rossi, K. Cheng, L. Khandker, K. Manova, and P. P. Pandolfi.** 2005. Role of Nucleophosmin in embryonic development and tumorigenesis. Nature **437:**147–153.
16. **Grisendi, S., and P. Pandolfi.** 2005. NPM mutations in acute myelogenous leukemia. N. Engl. J. Med. **352:**291–292.
17. **Herrera, J. E., R. Savkur, and M. O. Olson.** 1995. The ribonuclease activity of nucleolar protein B23. Nucleic Acids Res. **23:**3974–3979.
18. **Hinchcliffe, E. H., and G. Sluder.** 2002. Two for two: Cdk2 and its role in centrosome doubling. Oncogene **21:**6154–6160.
19. **Ishizaki, T., M. Maekawa, K. Fujisawa, K. Okawa, A. Iwamatsu, A. Fujita, N. Watanabe, Y. Saito, A. Kakizuka, N. Morii, and S. Narumiya.** 1996. The small GTP-binding protein Rho binds to and activates a 160 kDa Ser/Thr protein kinase homologous to myotonic dystrophy kinase. EMBO J. **15:**1885–1893.
20. **Ishizaki, T., M. Naito, K. Fujisawa, M. Maekawa, N. Watanabe, Y. Saito, and S. Narumiya.** 1997. p160ROCK, a Rho-associated coiled-coil forming protein kinase, works downstream of Rho and induces local adhesion. FEBS Lett. **404:**118–124.
21. **Ishizaki, T., M. Uehata, I. Tamechika, J. Keel, K. Nonomura, M. Maekawa, and S. Narumiya.** 2000. Pharmacological properties of Y-27632, a specific inhibitor of rho-associated kinases. Mol. Pharmacol. **57:**976–983.
22. **Kimura, K., M. Ito, M. Amano, K. Chihara, Y. Fukata, M. Nakafuku, B. Yamamori, J. Feng, T. Nakano, K. Okawa, A. Iwamatsu, and K. Kaibuchi.** 1996. Regulation of myosin phosphatase by Rho and Rho-associated kinase (Rho-kinase). Science **273:**245–248.
23. **Kondo, T., N. Minamino, T. Nagamura-Inoue, M. Matsumoto, T. Taniguchi, and N. Tanaka.** 1997. Identification and characterization of nucleophosmin/B23/numatrin which binds the anti-oncogenic transcription factor IRF-1 and manifests oncogenic activity. Oncogene **15:**1275–1281.
24. **Leung, T., X. Q. Chen, E. Manser, and L. Lim.** 1996. The p160 RhoA-binding kinase ROK alpha is a member of a kinase family and is involved in the reorganization of the cytoskeleton. Mol. Cell. Biol. **16:**5313–5327.
25. **Ma, Z., H. Izumi, M. Kanai, Y. Kabuyama, N. G. Ahn, and K. Fukasawa.** 2006. Mortalin controls centrosome duplication via modulating centrosomal localization of p53. Oncogene **25:**5377–5395.
26. **Matsui, T., M. Amano, T. Yamamoto, K. Chihara, M. Nakafuku, M. Ito, T. Nakano, K. Okawa, A. Iwamatsu, and K. Kaibuchi.** 1996. Rho-associated kinase, a novel serine/threonine kinase, as a putative target for small GTP binding protein Rho. EMBO J. **15:**2208–2216.
27. **Mazia, D.** 1987. The chromosome cycle and the centrosome cycle in the mitotic cycle. Int. Rev. Cytol. **100:**49–92.
28. **Morgan, D. O.** 1997. Cyclin-dependent kinases: engines, clocks, and microprocessors. Annu. Rev. Cell Dev. Biol. **13:**261–291.
29. **Moudjou, M., and M. Bornens.** 1998. Method of centrosome isolation from cultured animal cells, p. 111–119. *In* J. E. Celis (ed.), Cell biology: a laboratory handbook, 2nd ed., vol. 2. Academic Press, London, England.
30. **Mussman, J. G., H. F. Horn, P. E. Carroll, M. Okuda, L. A. Donehower, and K. Fukasawa.** 2000. Synergistic induction of centrosome hyperamplification by loss of p53 and cyclin E overexpression. Oncogene **19:**1635–1946.
31. **Nakagawa, O., K. Fujisawa, T. Ishizaki, Y. Saito, K. Nakao, and S. Narumiya.** 1996. ROCK-I and ROCK-II, two isoforms of Rho-associated coiled-coil forming protein serine/threonine kinase in mice. FEBS Lett. **392:**189–193.
32. **Okuda, M., H. F. Horn, P. Tarapore, Y. Tokuyama, A. G. Smulian, P. K. Chan, E. S. Knudsen, I. A. Hofmann, J. D. Snyder, K. E. Bove, and K. Fukasawa.** 2000. Nucleophosmin/B23 is a target of CDK2/cyclin E in centrosome duplication. Cell **103:**127–140.
33. **Okuwaki, M., A. Iwamatsu, M. Tsujimoto, and K. Nagata.** 2001. Identification of nucleophosmin/B23, an acidic nucleolar protein, as a stimulatory factor for in vitro replication of adenovirus DNA complexed with viral basic core proteins. J. Mol. Biol. **311:**41–55.
34. **Palaniswamy, V., K. C. Moraes, C. J. Wilusz, and J. Wilusz.** 2006. Nucleophosmin is selectively deposited on mRNA during polyadenylation. Nat. Struct. Mol. Biol. **13:**429–435.
35. **Reed, S. I.** 1997. Control of G1/S transition. Cancer Surv. **29:**7–23.
36. **Sanders, M. A., and J. L. Salisbury.** 1994. Centrin plays an essential role in microtubule severing during flagellar excision in Chlamydomonas reinhardtii. J. Cell Biol. **124:**795–805.
37. **Sebbagh, M., C. Renvoize, J. Hamelin, N. Riche, J. Bertoglio, and J. Breard.** 2001. Caspase-3-mediated cleavage of ROCK I induces MLC phosphorylation and apoptotic membrane blebbing. Nat. Cell Biol. **3:**346–352.
38. **Shinmura, K., P. Tarapore, Y. Tokuyama, K. R. George, and K. Fukasawa.** 2005. Characterization of centrosomal association of nucleophosmin/B23 linked to Crm1 activity. FEBS Lett. **579:**6621–6634.
39. **Spector, D. L., R. L. Ochs, and H. Busch.** 1984. Silver staining, immunofluorescence, and immunoelectron microscopic localization of nucleolar phosphoproteins B23 and C23. Chromosoma **90:**139–148.
40. **Szebeni, A., B. Mehrotra, A. Baumann, S. A. Adam, P. T. Wingfield, and M. O. Olson.** 1997. Nucleolar protein B23 stimulates nuclear import of the HIV-1 Rev protein and NLS-conjugated albumin. Biochemistry **36:**3941–3949.
41. **Szebeni, A., and M. O. Olson.** 1999. Nucleolar protein B23 has molecular chaperone activities. Protein Sci. **8:**905–912.
42. **Takemura, M., K. Sato, M. Nishio, T. Akiyama, H. Umekawa, and S. Yoshida.** 1999. Nucleolar protein B23.1 binds to retinoblastoma protein and synergistically stimulates DNA polymerase alpha activity. J. Biochem. (Tokyo) **125:**904–909.
43. **Tarapore, P., H. F. Horn, Y. Tokuyama, and K. Fukasawa.** 2001. Direct regulation of the centrosome duplication cycle by the p53–p21 (Waf1/Cip1) pathway. Oncogene **20:**3173–3184.
44. **Tarapore, P., K. Shinmura, H. Suzuki, Y. Tokuyama, S. H. Kim, A. Mayeda, and K. Fukasawa.** 2006. Thr199 phosphorylation targets nucleophosmin to nuclear speckles and represses pre-mRNA processing. FEBS Lett. **580:**399–409.
45. **Thumkeo, D., J. Keel, T. Ishizaki, M. Hirose, K. Nonomura, H. Oshima, M. Oshima, M. M. Taketo, and S. Narumiya.** 2003. Targeted disruption of the mouse rho-associated kinase 2 gene results in intrauterine growth retardation and fetal death. Mol. Cell. Biol. **23:**5043–5055.
46. **Tokuyama, Y., H. F. Horn, K. Kawamura, P. Tarapore, and K. Fukasawa.** 2001. Specific phosphorylation of nucleophosmin on Thr(199) by cyclin-dependent kinase 2-cyclin E and its role in centrosome duplication. J. Biol. Chem. **276:**21529–21537.
47. **Totsukawa, G., Y. Yamakita, S. Yamashiro, D. J. Hartshorne, Y. Sasaki, and F. Matsumura.** 2000. Distinct roles of ROCK (Rho-kinase) and MLCK in spatial regulation of MLC phosphorylation for assembly of stress fibers and focal adhesions in 3T3 fibroblasts. J. Cell Biol. **150:**797–806.
48. **Valdez, B. C., L. Perlaky, D. Henning, Y. Saijo, P. K. Chan, and H. Busch.** 1994. Identification of the nuclear and nucleolar localization signals of the protein p120. Interaction with translocation protein B23. J. Biol. Chem. **269:**23776–23783.
49. **Wang, W., A. Budhu, M. Forgues, and X. W. Wang.** 2005. Temporal and spatial control of nucleophosmin by the Ran-Crm1 complex in centrosome duplication. Nat. Cell Biol. **7:**823–830.
50. **Yoneda, A., A. B. Multhaupt, and J. R. Couchman.** 2005. The Rho kinases I and II regulate different aspects of myosin II activity. J. Cell Biol. **170:**443–553.
51. **Yung, B. Y., H. Busch, and P. K. Chan.** 1985. Translocation of nucleolar phosphoprotein B23 (37 kDa/pI 5.1) induced by selective inhibitors of ribosome synthesis. Biochim. Biophys. Acta **826:**167–173.